Journal of Pharmaceutical and Biomedical Analysis 55 (2011) 1–15

Contents lists available at ScienceDirect

Journal of Pharmaceutical and Biomedical Analysis

journal homepage: www.elsevier.com/locate/jpba

Review

NMR techniques in biomedical and pharmaceutical analysis

M. Malet-Martino [a,*], U. Holzgrabe [b]

[a] Groupe de RMN Biomédicale, Laboratoire SPCMIB (UMR CNRS 5068), Université de Toulouse, 118 Route de Narbonne, 31062 Toulouse cedex, France
[b] Institute of Pharmacy and Food Chemistry, University of Würzburg, Am Hubland, 97074 Würzburg, Germany

ARTICLE INFO

Article history:
Received 1 November 2010
Received in revised form
12 December 2010
Accepted 15 December 2010
Available online 23 December 2010

Keywords:
In vitro NMR
In vivo NMR
Metabolomics
Brain tumor grading
Drug analysis

ABSTRACT

This article focuses on the description of some of the NMR techniques used in the field of biomedical and pharmaceutical research. Indeed, the NMR method has special characteristics which make it uniquely suitable for these kinds of studies. It is non-selective so that all the low molecular weight compounds in the sample investigated are detected simultaneously in a single run. NMR also provides rich structural information which is an important asset to characterize complex mixture components. NMR is quantitative, i.e. the area of a NMR signal is directly proportional to the number of corresponding nuclei and thus, at variance with other techniques, the response factor is not dependent on the molecular structure. It is also a non-invasive tool that permits *in vivo* studies in humans. Compared with other techniques, NMR is significantly insensitive, which represents the main drawback of the technique. The recent technological developments of the technique have nevertheless considerably improved its sensitivity.

The first part of this article presents an overview of the advantages and limitations of NMR for *in vitro* quantitative analysis of complex matrices in liquid or semi-solid phases. The second part deals with the NMR-based metabolomics methodology. The third part describes the *in vivo* clinical magnetic resonance spectroscopy techniques. The fourth part reports some examples of NMR applications in the biomedical and pharmaceutical research fields.

Contents

1. Introduction 2
2. Advantages and limitations of NMR for *in vitro* quantitative analysis of complex mixtures 2
   2.1. Absolute quantification 2
   2.2. Sensitivity 3
3. NMR-based metabolomics 3
4. *In vivo* magnetic resonance spectroscopy (MRS) techniques 4
   4.1. Localization and spectral data acquisition 5
   4.2. Quantitative *in vivo* MRS 6
      4.2.1. Post-processing, resonance assignment and peak area measurement 6
      4.2.2. Absolute quantification 6
5. Applications 7
   5.1. MRS/NMR applications in the biomedical field 7
   5.2. NMR applications in pharmaceutical analysis 10
      5.2.1. Purity control of amino acids 11
      5.2.2. Identity control of small peptides 12
      5.2.3. Quality control of heparin derivatives 12
6. Conclusion 12
   References 12

* Corresponding author. Tel.: +33 5 61 55 68 90.
E-mail address: martino@chimie.ups-tlse.fr (M. Malet-Martino).

0731-7085/$ – see front matter © 2010 Elsevier B.V. All rights reserved.
doi:10.1016/j.jpba.2010.12.023

1. Introduction

Nowadays, about 65 years after the observation of proton nuclear magnetic resonance (^{1}H NMR) in liquid water and paraffin wax respectively by research groups led by Bloch at Stanford University and Purcell at Harvard University [1–3], NMR spectroscopy is the preeminent method for determining the structures of synthesized and natural compounds, including the three-dimensional structures of proteins and other macromolecules in solution. However, NMR has also found many applications in other fields than chemistry, such as food science, biology, pharmacy and medicine since it is the only physical method used routinely that can provide quantitative valuable information at the molecular level, regarding analysis of complex mixtures from fluids of biological origin, food materials, beverages, drugs, cell or tissue extracts, excised tissues, cell pellets (*in vitro* studies) to isolated perfused biological systems (cell or organs) (*ex vivo* studies) [4–15] and finally intact living systems (bacteria, plants, animals and humans) (*in vivo* studies) [16–20].

Consequently, NMR is unique in its ability to perform analyses in the field of biomedical and pharmaceutical research. This article will focus on the description of some of the NMR techniques used in these domains and their applications. The first part presents an overview of the advantages and limitations of NMR for *in vitro* quantitative analysis of complex matrices in liquid or semi-solid phases. The second part deals with the NMR-based metabolomics methodology. The third part describes the *in vivo* clinical magnetic resonance spectroscopy techniques. The fourth part reports some examples of NMR applications in the biomedical and pharmaceutical research fields.

2. Advantages and limitations of NMR for *in vitro* quantitative analysis of complex mixtures

NMR is non-invasive and non-destructive so that the sample is available for subsequent analysis by an alternative technique. NMR enables the direct study of intact biofluids and semi-solid or solid samples (e.g. intact cells or tissues, drugs) using magic-angle spinning (MAS) methodology. As solids give generally broad lines, conventional high-resolution NMR is a liquid-phase based technique with signal width lines at half-height usually of a few Hz. However, with the development of high resolution-MAS (HR-MAS) NMR, spectra of whole cells or small pieces of intact tissues can be obtained with a resolution comparable to that of homogeneous solutions although intrinsically a little bit lower. Indeed, the high rate spinning of the semi-solid samples at the magic angle of 54.7° with respect to the static magnetic field considerably reduces signal broadening effects due to chemical shift anisotropy and dipolar coupling, but not those related to the magnetic susceptibility gradients across the small specimen analyzed [21]. Moreover, whatever the native physical state (solid or liquid) of the sample investigated, its NMR solution requires minimal preparation (respectively dissolution or dilution in an adequate deuterated solvent).

The NMR method has special characteristics which make it uniquely suitable for the analysis of mixtures. It is non-selective so that all the low molecular weight compounds in the solution/sample (provided they bear the nucleus under investigation and are present at sufficient concentrations) are detected simultaneously in a single run. There are several magnetically active nuclei that can be routinely used for the analysis of biological or pharmaceutical mixtures: ^{1}H (the most sensitive), carbon-13 (^{13}C), fluorine-19 (^{19}F), phosphorus-31 (^{31}P).

NMR also provides rich structural information. Indeed chemical shifts, multiplicity, integrals as well as homo- and heteronuclear two- or three-dimensional (2D or 3D) experiments such as COSY, TOCSY, HSQC, HMBC, NOESY, ROESY, HSQC-TOCSY, HMBC-TOCSY, etc., make up a powerful toolkit to probe the molecular structure of complex mixture components.

2.1. Absolute quantification

The area (referred to as the intensity or the integral) of a NMR signal is directly proportional to the number of corresponding nuclei and thus, at variance with other techniques, the response factor is not dependent on the molecular structure. This is only true under well-defined experimental conditions. Indeed for quantitative measurements, the spectra must be acquired and processed under appropriate conditions [12,22]. First, it is necessary to check that the entire spectral width (SW) is uniformly excited by the radiofrequency (RF) pulse when resonances extend over a wide range as with ^{13}C, ^{19}F or ^{31}P nucleus. Second, concerning data collection, there are some features to take into account. To avoid artificial distortions of the signal intensities, the spectra must be recorded (i) using a repetition time (TR), also called recycling time, of at least five times the longitudinal relaxation time (T_1) (after a 90° excitation pulse) of the slowest relaxing nucleus, which allows the spins to be fully relaxed and (ii) with an adequate digitization so that the NMR lines are described with more than five data points above their half-height (e.g. 32 K for ^{1}H or more if a large SW needs to be used). Moreover, when heteronuclear NMR spectra are recorded with broadband ^{1}H decoupling, the intensity of the signals must be corrected for the Nuclear Overhauser Enhancement (NOE) distortions or these distortions suppressed by using inverse-gated recording conditions (^{1}H decoupling applied only during the acquisition time). Third, the data processing must be optimized (zero-filling, apodization by a window function, careful correction of phase and baseline distortions of the spectrum) to enhance the definition of the lineshape and improve the resolution or the signal-to-noise ratio (S/N). Integration of the peak areas can then be performed. Its accuracy is greatly dependent on the S/N of the peak considered. A S/N of at least 150 is required for an uncertainty of ≈1%, but an acceptable level of precision, ≈3% and 8%, is obtained for S/N ≈30 and 10, respectively [23].

The measurements of absolute concentrations involve the presence in the spectrum of a reference signal of known concentration to provide a calibration standard. In solutions, the concentrations of the analytes are calculated by comparing the analyte and reference integrals corrected from the number of contributing nuclei in their respective resonances. One can use an internal or external reference contained in a coaxial capillary put into the larger NMR tube, if a contamination of the sample analyzed with the reference needs to be avoided. Both of them have to satisfy several constraints which are well described elsewhere (e.g. [24,25]). However, it is impossible to find a universal reference substance for quantitative (even for one type of nucleus) measurements and a number of possible reference compounds for ^{1}H, ^{19}F and ^{31}P NMR are listed in Refs. [26,27]. Applying all the requirements given above, assay determinations with uncertainty of approximately 1% are achieved so long as the integration limits are extended over a frequency range of 64 times the full width at half signal height to ensure than >99% of the whole signal intensity is recovered [23]. This is difficult to fulfill due to adjacent or overlapped peaks, especially in complex mixtures, even if the signal separation can be optimized by changing the solvent or using a combination of solvents in pharmaceutical preparations or modifying the pH value of the biological samples [e.g. 14,27]. For instance, the ^{1}H NMR assay of the well-isolated or resolved but closed resonances of glutamine, glycerophosphocholine (GPC), phosphocholine (PC), choline (Cho) and creatine (Cr) in the 2.9–3.8 ppm spectral region in a model D_2O solution at concentrations between 0.03 and 2.0 mM was performed with a precision in the range 2–7% and an accuracy within ±7% of the nominal concentration value [14]. In biofluids,

cell or tissue extracts as well as whole cells or intact tissues (using HR-MAS probes) analyzed with currently available high-field spectrometers (500–800 MHz), all the signals are not well-resolved and overlap of a number of resonances still remains. Therefore, deconvolution algorithms have to be applied to resolve and quantify the signals. The quantification of the metabolites is performed using semi-automatic or automatic routine softwares fitting signals of reference standards to the experimentally acquired data [28–31]. 2D NMR TOCSY technique is also successfully used to resolve and quantify, through the measurement of their cross-peak volumes, most of the metabolite resonances that are heavily overlapped in one-dimensional (1D) ^{1}H spectra [32–35].

In biological samples, quantitation may be affected by the binding of metabolites and/or internal reference to endogenous components such as macromolecules in blood plasma or serum, or by micellar substructures in bile. This results in significant broadening that leads to reduced S/N or even to NMR invisibility of the signals concerned. Some sample pretreatment may be therefore required as for example proteins and macromolecules removal from blood plasma or serum which can be performed by extraction methods or ultrafiltration [36,37]. Absolute metabolite quantitation in intact tissues using 1D HR-MAS ^{1}H NMR, beside the fulfillment of the prerequisites described above, requires that the integrated or computed peak areas are corrected for transversal relaxation T_2 decay during the echo delay when a CPMG spin echo sequence is employed to suppress broad spectral components [38,39]. Moreover, the addition of known amounts of classical internal chemical proton reference standards used in aqueous solutions (trimethylsilyl-2,2,3,3-d_4-propionic acid sodium salt (TSP) or 4,4-dimethyl-4-silapentane-1-sulfonic acid sodium salt (DSS)) to the biopsy sample leads to overestimation of metabolite concentrations as they can bind significantly to tissue components and flow out of the RF coil detectable volume, thus becoming partly invisible, which would cause an overestimation of metabolite concentrations if used as a reference [40–42]. As an example, only 27.5% of the TSP amount that was expected based on the mass of TSP added to the sample was detected in human prostate tissue specimen [41]. The Electronic Reference To access *In vivo* Concentrations (ERETIC^{TM}) technique which uses a synthesized RF pulse to produce an additional peak in the spectrum is the more convenient and accurate method for the determination of absolute metabolite concentrations in biopsy samples. However ERETIC is not routinely implemented on spectrometers [40,42].

2.2. Sensitivity

Compared with other techniques, in terms of the minimum sample amounts for an analysis, NMR is significantly insensitive, which represents the main drawback of the technique. Indeed, the limit of detection (LOD) of NMR ranges between 10^{-9} and 10^{-11} mol whereas laser-induced fluorescence reaches 10^{-13} mol, Fourier transform infrared spectroscopy and Raman spectroscopy 10^{-12} to 10^{-15} mol and mass spectrometry 10^{-19} mol [43].

To maximize the sensitivity (the S/N) of an NMR experiment, one can use (i) a static magnetic field as high as possible (resulting in a 1 GHz Larmor frequency for commercial supraconducting NMR spectrometers), (ii) cryoprobes (coils in which the noise voltage is reduced via the use of high-temperature supraconducting materials) allowing to lower the LOD by a factor 3–5 and (iii) a coil diameter (d) as low as possible down to ≈100 μm since the mass sensitivity increases with $1/d$ in a first approximation and below 100 μm with the square root of d [43].

Ten years ago, the following detection limits for ^{1}H nucleus in urine after ≈20–30 min of recording with 500 or 600 MHz spectrometers using conventional 5 mm probe and tube were reported by the group of Wevers: 5 and 10 μM respectively for the singlet and doublet resonances of methyl groups, 15 μM for the singlet and triplet resonances of methine and methylene groups respectively, 30 μM for the doublet resonance of methylene group [44,45]. It is very likely that the recent technological developments of the NMR technique have lowered the LOD of the method.

The total volume of sample required for NMR analysis in conventional 5 mm tube is 550 μL and 300 μL if a coaxial capillary is employed, but it is reduced to a few μL with microcoil probes (typically 5–30 μL) [46,47]. 1D ^{1}H NMR spectra of 10–15 μg of low molecular weight compounds (≈20–30 nmol) can be easily obtained in 10 min with high-field spectrometers in current use. Indeed, the mass sensitivity of the Bruker 1.7 mm TCI MicroCryoProbe^{TM} which utilizes 30 μL sample volume, is 14- and 6-fold greater than that of 5 and 3 mm conventional Bruker probes, respectively [48]. A comparative study of the performances of different Bruker TXI probes showed that the microliter probe is 5- and 1.7-fold more mass sensitive than the 5 mm conventional probe and cryoprobe, respectively, while its concentration sensitivity was found to be approximately 22- and 66-fold poorer, respectively. The cryoprobe is 3-fold more concentration sensitive than the conventional probe (Table 1) [46]. Another detailed sensitivity analysis demonstrated that the mass sensitivity of the Varian CapNMR probe with a flowcell volume of 5 μL is 10-fold greater than the conventional 5 mm probe, but, in contrast, the larger volume probe is 15-fold more concentration-sensitive [47]. In conclusion, direct NMR study of biological samples which are concentration-limited need to be performed in a 5 mm cryoprobe and conversely mass-limited samples are most effectively analyzed in a probe whose the observe coil is as small as permitted by the sample solubility.

3. NMR-based metabolomics

Since the pioneering work of Nicholson et al. [49], there has been an explosive growth in the application of metabolomics. Metabolomics or metabonomics, the two terms being often used interchangeably [50], is a field of study that attempts to detect all the low molecular weight organic metabolites in biofluids, cells, tissues or whole organisms, and applies chemometric methods to identify their key, but potentially subtle changes, as consequence of multiple context-dependent factors including genetics, diet, life-style, environment, disease state and pharmaceutical interventions. Hence, to perform metabolomics, it is necessary to generate comprehensive and representative metabolite profiles of complex biological samples. NMR (mainly ^{1}H NMR) is, with mass spectrometry (MS), the most accepted method used for metabolomic analyses. MS is intrinsically more sensitive than NMR but generally requires a chromatographic pre-separation step using gas-chromatography (GC) after chemical derivatization, liquid chromatography (LC) (high performance LC (HPLC) or ultra-pressure LC (UPLC)) or capillary electrophoresis (CE). Metabolomic studies are generally performed on biofluids (mostly urine and plasma or serum, but also a wide range of other fluids such as cerebrospinal fluid, ascitic fluid, bronchial washes, prostate secretions or cyst fluid) and cell, tissue or fecal extracts as well as whole cells or intact tissue specimens (e.g. biopsies, fine needle aspirates) using the HR-MAS technique.

The requirements for sample collection, storage and preparation including the extraction strategies are not discussed here and the interested reader can refer to the recent references of Beckonert et al. [51], Lin et al. [52], Tiziani et al. [36], Wu et al. [53], Issaq et al. [54] and Serkova and Glunde [37].

Three major steps can be defined in metabolomic analyses: first, the pattern recognition or group clustering based on spectral differences; second, the identification of the spectral regions that permits to distinguish sample classes and subsequently the specific metabolite(s) responsible for the group discrimination; third, the

Table 1
Comparison of Bruker probe performances (spectra were recorded on a Bruker DMX 600).

Probe	Fill volume V_{tot} (μL)	Active volume V_{obs} (μL)	Reported S/N for 0.5 μmol of sucrose in V_{tot} (NS = 1, LB = 1)	S_m[a] S/N per μmol in V_{obs}	Enhancement[b]	S_c[c] S/N per μmol L^{-1} in V_{tot}	Enhancement[b]
1 mm TXI microliter probe	5	2.5	276	1104	5	2760	1
5 mm conventional TXI	550	278	55	218	1	60,604	22
5 mm TXI cryoprobe	500	278	181	651	3	180,978	66

Adapted from [46].
[a] S_m: mass sensitivity. The obtained sensitivity was normalized to the signal-to-noise (S/N) ratio of 1 μmol of samples in the NMR active volume.
[b] Enhancement factors were given relative to conventional 5 mm probe for S_m and to 1 mm microliter probe for S_c.
[c] S_c: concentration sensitivity. Values were calculated from S_m values using the equation $S_c = V_{obs}S_m$ [47].

quantitation and validation of this (these) putative biomarker(s) with respect to a particular characteristic or outcome (e.g. physiological or pathological status, response to therapy).

^{1}H NMR spectra of biological samples consist of thousands of overlapping resonances and this enormous amount of raw data needs to be prepared to make them amenable to statistical analysis. This necessity has been fully discussed [55–57]. It typically involves the processing of acquired spectral data (phasing and polynomial baseline correction, removal of overdominating peaks such as the residual water peak after presaturation and urea in urine, peak alignment between the spectra), followed by data normalization (some form of adjustment of the intensity values measured either on each data point, on each peak or on segmented spectral regions that are referred to as variable values) and, if required, by data scaling of the variables. The spectral data are thus compiled in a matrix consisting of rows that identify samples and columns that represent variables.

The standard normalization method, integral normalization or normalization to constant sum (CS), expresses the intensity of each individual variable in a spectrum as a fraction of the summed integral intensity of this spectrum. Probabilistic quotient normalization (PQN) is an alternative approach. For each of the individual spectra, a series of quotients is generated by the element-wise division of the spectrum by a reference spectrum, typically a median spectrum [58]. Other methods also exist such as the histogram matching adapted from the field of image processing [59].

To improve and facilitate the subsequent statistical data analysis by reducing the number of variables, the spectra are divided along the chemical shift axis into regions called bins or buckets of constant width (from 0.01 to 0.1 ppm, typically 0.04 ppm) or adaptive width (intelligent bucketing in which the bin edges correspond to minima in the spectrum). The total peak intensity within each bucket is summed providing a characteristic integral of one variable.

Given the high dynamic range of metabolite concentrations in biological samples, a normalization on the columns of data (i.e. on each spectral intensity of a variable across all samples) is recommended to avoid that changes in abundant metabolites dominate statistical models. Three classes of methods (centering, scaling and transformations) are most commonly used. Centering or mean centering that converts each value intensity to fluctuations around zero instead of around the mean of all the column values, is applied in combination with transformation (non linear conversion of the data, most often logarithmic) or scaling methods such as autoscaling (also called variance scaling, unit scaling or unit variance scaling) or Pareto scaling that divides each value in the column by the standard deviation (SD) of the column or the square root of the SD of the column, respectively [60]. The data sets obtained at this stage are then submitted to statistical modeling for pattern recognition using unsupervised and supervised methods. Unsupervised data analysis, such as Principal Component Analysis (PCA) or hierarchical cluster analysis, maps samples according to their properties without knowledge of their class and then establishes whether or not any intrinsic clustering exists within a sample group. Supervised methods, such as Partial Least Squares-Discriminant Analysis (also known as Projection to Latent Structures-Discriminant Analysis) (PLS-DA), Orthogonal Projection to Latent Structures-DA (O-PLS-DA) or neural networks, use prior class information to optimize the separation between two or more sample classes. PCA, PLS-DA and O-PLS-DA methods are widely used for NMR-based metabolic profiling [61].

Identification of the metabolites at the origin of the samples group clustering can be accomplished using free web-based and commercial NMR spectral libraries as the Human Metabolome Database (HMDB) [62], the Madison Metabolomics Consortium Database (MMCD) [63], the Biological Magnetic Resonance Data Bank (BMRB) [64], the Magnetic Resonance Metabolomics Database [65] or the Chenomx database [66], as well as open source or not publicly available software tools (e.g. Analysis of MIXtures (AMIX) program [67], MetaboMiner [68] or rNMR which also permits to quantify the metabolites [69]). The statistical total correlation spectroscopy (STOCSY) is a new approach to molecular identification in a complex mixture. The method exploits the colinearity of many of the intensity variables in a set of spectra (as ^{1}H NMR spectra) to generate a pseudo-2D NMR spectrum (resembling TOCSY) that displays the correlation among the intensities of the various peaks. Strong correlations between spectral intensities lead to identification of resonances from the same molecule, even with no NMR-based spin-coupling connectivity. Connections between peaks belonging to different molecules involved in the same metabolic pathway can be detected by examining lower coefficients or even negative correlations [70,71].

The statistical approach for the validation of putative metabolite markers between the different groups can be represented by a standard Student's *t*-test or analysis of variance (ANOVA) [72].

4. *In vivo* magnetic resonance spectroscopy (MRS) techniques

In the context of human (and by extension animal) *in vivo* studies, NMR spectroscopy is commonly referred to as MRS to avoid the upsetting word "nuclear" when talking to human volunteers or patients as it may erroneously lead to associations with radioactive materials and/or ionizing radiation and also because the technique involves the use of the same scanners than those employed to carry out magnetic resonance imaging (MRI) investigations.

A number of magnetically active nuclei found in biological systems (^{1}H, ^{13}C, sodium-23 (^{23}Na), ^{31}P) or in xenobiotics (lithium-7 (^{7}Li), ^{19}F) are available for *in vivo* MRS studies. However, mainly the ^{1}H nucleus is used for practical applications in biomedicine since it has favorable NMR characteristics (nuclear spin of 1/2, almost 100% natural abundance, highest sensitivity of any stable nucleus) and it is present in nearly all the metabolites and also because the ^{1}H MRS spectra can be performed using clinical MRI scanners with no additional hardware required.

Conventional MRI measures the intensity of the resonances of all hydrogen-bearing moieties (roughly the proton density) contained in the volume of tissue excited by the RF pulse. The human body

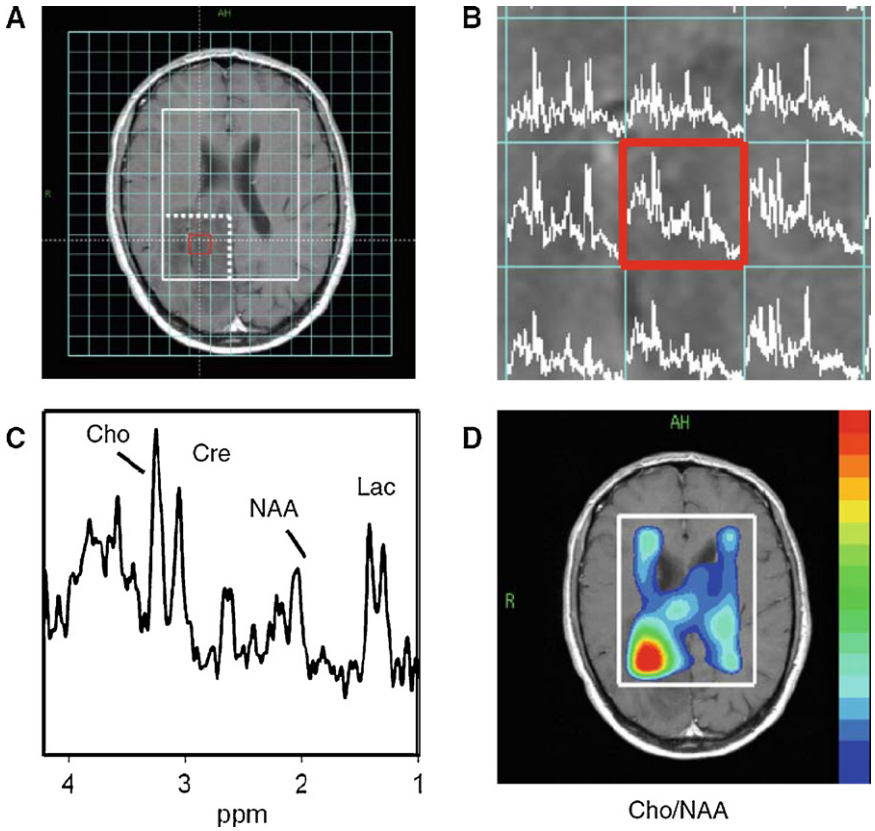

Fig. 1. MRSI data obtained from a patient with a brain tumor. A: MR image with VOI selected by STEAM in white. Spectra are only acquired from the MRSI voxels inside the VOI. The dotted line in A indicates the MRSI voxels shown in B. B: Part of the spectral image showing MRSI voxels with their corresponding spectra. C: Enlargement of the spectrum obtained from the voxel indicated in red in A and B. D: Metabolite map showing the intensity distribution of the ratio of choline (Cho) to N-acetylaspartate (NAA) over the VOI with the highest intensity indicated in red at the position of the tumor. Cre: creatine, Lac: lactate. (For interpretation of the references to color in this figure legend, the reader is referred to the web version of the article.)
Adapted from [86].

is primarily water and fat. In consequence, the high signal intensity of water and methylene lipid groups is used to obtain detailed anatomical images by assigning shades of gray, white and black to the strength of their signals. As in CT (Computed Tomography) scanners, the signals are subdivided into tiny cubes or rectangular volumes called voxels (volume elements). Each of them has different signal intensity and is therefore made of different shade. The image is thus composed of a sum of voxels or pixels (picture elements) whose size is typically 1 mm × 1 mm × 5 mm or less. In MRS, the signals of interest are not those of water and lipids but rather those of metabolites which are approximately 10,000 times less concentrated. Indeed, the concentration of endogenous metabolites ranges between 1 and 30 mM in hydrogen, typically 10 mM, whereas that of water is approximately 80 M in hydrogen. Hence, the detection of their resonances requires a magnetic field strength of 1.5 Tesla (T) (which corresponds to ≈65 MHz for the resonance of proton) or higher, while clinical magnetic resonance (MR) images can be obtained with magnetic field strength as low as 0.2 T. Today, 1.5 T MR scanners and well over a thousand of 3 T MR systems are commonly used for clinical routine. Ultra high field MR scanners (≥7 T) are available for clinical research (more than thirty operating at 7 T and a few ones at 9.4 T) as well as for biomedical research on small animals at field strengths up to 20 T and commonly at 9.4 and 14.1 T [73].

For biological tissues, the enhancement of S/N and chemical shift resolution with increasing magnetic field strength (B_0) may be less than the predicted linear improvement. This appears to be due to the line width increase with B_0. Nevertheless, it is clearly demonstrated that S/N and resolution in spectra at 3 T or 7 T are improved compared to those at 1.5 T or 4 T, respectively [74–77]. Hence, higher field strength MR systems permit detecting moieties at lower concentrations, reducing resonance overlap and decreasing the voxel volume that can be observed.

The high intensity of water and lipid resonances at 4.8 and 1.3 ppm respectively overwhelm all the resonances of the metabolites of interest (dispersed between 0 and 4.8 ppm) whose intensity is far below (several orders of magnitude). Therefore, suppression techniques of these signals are critical in order to reliably observe the much smaller metabolite signals. The most common approaches to suppress the water signal prior the start of the localization sequence are the CHEmical Shift-Selective (CHESS) sequence which presaturates the water signal using frequency-selective 90° pulses [78] and the Water suppression Enhanced through T_1 effects (WET) that utilizes selective excitation of the water resonance followed by dephasing gradients [79]. It is also possible to suppress water and lipid resonances during the localization sequence through the use of frequency-selective inversion (180°) pulse surrounded by a spoiler gradient pulse of opposite signs, a method known as "MEGA" or "double BASING" (BAnd Selective INversion with Gradient dephasing) [80–82].

4.1. Localization and spectral data acquisition

In vivo MRS examination starts with the identification of a spatially well-defined tissue volume called Volume Of Interest (VOI) which can be described by a voxel or voxels. The sizes of the voxels used for MRS studies with current MR systems (1.5 or 3 T) are generally in the range 3–8 cm^3, however voxels as small as 1 cm^3

may be selected (e.g. [75,76,83]). The spatial localization is performed using either Single-Voxel Spectroscopy (SVS) which records the spectrum from a single region, or Magnetic Resonance Spectroscopic Imaging (MRSI), originally introduced as Chemical Shift Imaging (CSI) by Brown et al. [84], in which the volume investigated is divided in multiple smaller voxels, the spectra of each of them being acquired simultaneously. Hence, the technique allows determining the spatial distribution of various metabolites in a single experiment (Fig. 1). The basic principles and methodology of MRSI are well presented elsewhere (e.g. [75,85,86]). Two commonly used techniques for localization and interrogation of a voxel or voxels are Point-Resolved Spatially localized Spectroscopy (PRESS) [87] and STimulated Echo Acquisition Mode (STEAM) [88]. Both of them involve sequential application of three orthogonal gradients to select slices, during which selective RF pulses (three 90° pulses in STEAM and a 90° pulse followed by two 180° pulses in PRESS) are applied and generate a spin echo. Hence, at the end of the three-slice series, only the signal from the spins within the chosen volume (voxel(s)) is refocused and acquired. Changing the delay times between the pulses modify the echo time (TE). Using a longer TE decreases the signal intensity due to T_2 relaxation and changes the phase of the multiplet signals due to J-coupling modulation. Signals with minimal intensity loss due to T_1 and T_2 relaxations are obtained by acquiring the spectra with a long TR combined with a short TE. Conversely, the spectra recorded with long TR and TE contain only resonances of metabolites with high T_2 values whereas those of the compounds with short T_2 are dephased, becoming thus undetectable. The principal advantage of PRESS over STEAM is the additional gain in S/N with the collection of a spin echo as opposed to a stimulated echo. Indeed, half of the signal is not used in acquisition of a stimulated echo, resulting in a 50% signal intensity loss. On the other hand, the presence of two 180° pulses in the PRESS sequence does not allow performing data acquisition with very short TE; they result in a poor sharpness of edges of voxel and thus a not optimal volume selection, and in a chemical shift displacement error, which increases with the magnetic field strength, larger than with the STEAM sequence. However, these disadvantages have been lowered with the improvement of 180° pulse designs or the replacement of each 180° pulse by two adiabatic pulses (e.g. [86]). STEAM and PRESS are currently used for short and long TE data acquisitions (e.g. [89,90]). In MRSI, both PRESS and STEAM sequences can be applied with phase-encoding gradients which allow the defined volumes to be subdivided. However, MRSI data can also be collected without PRESS or STEAM localization and a number of alternative strategies have been proposed to reduce acquisition time, increase spatial resolution or extend the field of view (e.g. [75,85]). The main disadvantage of MRSI is the contamination of the spectrum of a voxel by signals originating from adjacent voxels, the so-called voxel bleed [86].

4.2. Quantitative in vivo MRS

As for *in vitro* NMR quantification, two steps need to be considered: first, the determination of accurate peak areas and their assignments to relevant metabolites, and second, conversion of the peak areas into metabolite concentration using adequate calibration references.

4.2.1. Post-processing, resonance assignment and peak area measurement

In vivo MRS post-processing is basically not different from that use in high-resolution NMR. It includes apodization, zero-filling, Fourier transform (FT), phasing and baseline correction. However, it must be taken into account that in localized MRS, the rapid gradient switching produces electric currents known as eddy currents that are time- and space-dependent, causing shifts of the resonance frequency which result in distortion of the spectrum after FT. Such artifacts can be removed using the water signal collected without water suppression as a reference to correct for frequency and line shape variations in the metabolite spectrum. Most modern MRI systems are equipped with actively shielded gradients that minimize the effect of eddy currents. Although less essential, eddy current correction is still commonly used for automatic phasing and frequency offset correction [86].

The identification and assignment of resonances may be accomplished in several ways. First, spectra may be acquired by using phantoms that contain compounds thought to be present in the tissue under investigation using the same experimental parameters. Large database established from *in vitro* measurements are available to assist the process of metabolite identification (e.g. [91]). Second, spectra may be acquired with different TEs to provide information about the T_2 values of the resonances and to reveal their multiplicities. Third, more sophisticated MR experiments such as "editing" and 2D correlation spectroscopy may be performed *in vivo* to obtain a more precise assignment of resonances to specific molecules [92,93]. At the low field strengths (1.5 and 3 T) commonly used for clinical MRS investigations (compared to field strengths of 11.8–18.8 T (500–800 MHz) currently utilized for *in vitro* NMR analysis), there is a considerable resonance overlap which precludes any integration of individual metabolite resonances and the determination of the intensity resonance requires spectral deconvolution using fitting programs. The most accurate data are obtained with peak fitting routine incorporating prior knowledge about the metabolites that contribute to the MRS signal [94]. The LCModel™ (Linear Combination of Model spectra) developed by Provencher [95] is a widely used software package for the automatic quantification of ^{1}H *in vivo* MRS spectra as well as ^{1}H *in vitro* HR-MAS NMR spectra. The model fits spectra as Linear Combination of Model spectra from 23 relevant metabolites and 18 simulated lipids and macromolecules peaks in the version 6.1-4. It is very truthful for the evaluation of brain spectra acquired with short TE and hence containing many overlapping resonances. Conversely, the quantification package jMRUI (Java-based Magnetic Resonance User Interface) [96] which fits the data in the time domain using prior knowledge of the metabolite resonance parameters, is generally used for quantification of spectra obtained with long TE and thus with fewer overlapping signals. These two software programs allow not only to determine the signal intensities but also give information on the quality of the fit with the Cramér-Rao lower bound as an error estimation [86]. An extensive description of currently used computer programs for the analysis of *in vivo* ^{1}H MRS spectra can be found in the publication of Jansen et al. [94].

4.2.2. Absolute quantification

The area of a peak is directly proportional to the number of nuclei that contribute to it and to the concentration of the metabolite to which the nuclei belong. However, the peak areas depend on several factors such as receiver gain instability, compartmentation or MR visibility of metabolites whose influence is described in detail by Jansen et al. [94] as well as T_1 and T_2 relaxation times. To avoid a reduction of the signal intensity, the spectra must be recorded with a TR longer than five times the T_1 of the relevant metabolites. As an example, the T_1 of the methyl protons of N-acetylaspartate (NAA) being ≈1400 ms at 1.5 T, using a TR of 2000 ms leads to a decrease of its signal intensity of ≈25%, whereas with a TR of 7000 ms, the reduction is less than 1% [94]. Therefore, when the TR does not fulfill this condition, the peak area of the metabolites should be corrected for partial saturation separately as their T_1 values are not the same.

Recording the spectra with a short TE (6–30 ms) minimizes signal loss due to T_2 relaxation. Indeed, the reduction of the signal intensity of the NAA methyl group (T_2 ≈ 400 ms at 1.5 T) is ≈5% if a

TE of 20 ms is used and ≈21% when the TE is 100 ms. However, the signal intensity of compounds with very short T_2, such as macromolecules ($T_2 \approx 50$ ms), is significantly reduced even with a short TE (≈33% macromolecule signal loss with a TE of 20 ms). On the other hand, spectra acquired with a long TE (≥135 ms) have less complicated appearance since the signals of metabolites with short T_2 are highly reduced or even not detectable [94]. Therefore, signal intensities of each resonance have to be corrected for T_2 relaxation according to the TE value used. However, it is not conceivable to correct each signal intensity for relaxation effects as each metabolite in each patient has its own T_1 and T_2 values and their determination is too time-consuming to be performed in every patient. It is therefore better to acquire spectra with long TR and TE as short as possible to minimize the reduction of the signal intensities.

Signal intensities (possibly corrected for relaxation effects) determined using the data analysis procedures are expressed in arbitrary units, with ratios widely and successfully applied in the clinical diagnosis of pathological tissues. With this approach, one of the measured peaks whose concentration is supposed to be invariant serves as a reference standard and is used as the denominator in the peak ratios. However, even if the reference metabolite peak area is measured in healthy tissue, it remains uncertain if this hypothesis is correct and the alterations observed in the peak ratio can be caused by variations in the concentration of the numerator only (what is expected), the denominator or both. Peak areas of all the metabolites can be converted into concentrations by using a value from the literature for the reference metabolite concentration. Although concentration values in mmol/kg wet weight can thus be obtained, this remains a relative quantification method. To overcome this limitation, absolute quantification of metabolites can be determined. It requires referencing to an internal or external standard of known concentration. Tissue water signal is frequently used as an internal reference. Two spectra are successively recorded on the same voxel, with and without presaturation of the water signal. Because the MRS determination of the water content is difficult, one usually applies a value from the literature taking into account that this value varies according to the pathology [97]. Some quantification strategies using an external reference have been developed [94]. The signal intensity of the metabolites is then correlated to that of a known amount of the external standard which is present inside the coil at the time of the *in vivo* measurement (external standard method) or which is placed at the position of the patient afterwards (replace-and-match method). Jansen et al. [94] in an excellent and comprehensive review on *in vivo* MRS quantification strategies reported that the replace-and-match method is the most accurate but requires extra-imaging and preparation times and is not easy to use, whereas external reference and internal water referencing methods are less accurate, need extra-imaging time and for the former is not easy to use. Very recently, the applicability of the ERETIC method in a clinical environment was demonstrated. The method has been improved to enable accurate and reproducible quantification *in vivo* on a 3 T MR system. The metabolite concentrations measured in healthy volunteers were in good agreement with literature values and with internal water referencing [98].

5. Applications

5.1. MRS/NMR applications in the biomedical field

We elected to focus our examples to the application of MRS and NMR to brain tumor studies because there is a large body of work that has concentrated on these tumors. For more general applications, the reader can consult for instance the excellent and recent reviews of Soares and Law [99], van der Graaf [86] and DeFeo and Cheng [100].

There are two types of brain tumors: primary brain tumors that originate in the brain and metastatic (secondary) brain tumors that originate from cancer cells that have migrated from other parts of the body. In adults, the most common types of cancer that spread to the brain are melanoma, breast cancer, renal cell carcinoma and colorectal cancer. The overall incidence rate for primary brain and central nervous system (CNS) tumors in European countries and United States depends on age and is approximately 18 cases/100,000 persons per year [101]. Even if one-quarter of the cost of care for cancer patients is allocated for CNS tumors, survival rates are still very poor in all countries.

Gliomas account for more than 90% of primary brain tumors in patients older than 20 years and for more than 60% of all intracranial brain tumors in all patients [101]. Gliomas are named according to the specific type of cell from which they originate. The main types of gliomas are astrocytomas that specifically arise from astrocytes and include the highly malignant glioblastoma multiforme (GBM), oligodendrogliomas originating from oligodendrocytes, and mixed oligoastrocytomas coming from both astrocytes and oligodendrocytes [102]. Gliomas are further categorized according to their grade that is defined according to the WHO classification [103]. Low-grade (LG) gliomas (WHO grade I–II) are well-differentiated, i.e. not anaplastic; these are not benign but still portend a better prognosis for the patient. High-grade (HG) gliomas (WHO grade III–IV) are undifferentiated, i.e. anaplastic; these are malignant and carry a worse prognosis [103].

The grading of a tumor has important implication for clinical management because the grade of the tumor defines to a substantial extent survival probability and course of therapy. The gold standard of tumor grading is histopathological diagnosis requiring a biopsy during an open or stereotactic neurosurgical procedure. However, the technique has limitations due to sampling errors, inter- and intra-observer variability and the intrinsic heterogeneity of cerebral gliomas that may confound histopathological diagnoses made on small biopsy specimens [104,105]. Moreover, the histopathological classification of gliomas is complex and still under discussion and revision [106]. This stresses the interest of an additional and/or alternative technique that does not resort to any invasive act. ^{1}H MRS has thus been proposed as a risk free method for grading cerebral gliomas and numerous studies have been conducted in this aim. We focus here on the most recent studies as literature data up to 2004 have been reviewed by Hollingworth et al. [107].

Non-invasive grading of gliomas still remains a challenge as clear conclusions have not yet been drawn mainly due to the different techniques employed, the size of the voxel(s) analyzed, the lack of consensus regarding the best metabolite(s) to be taken into account, the methods for metabolite quantification and the choice of the cohorts of patients evaluated.

Numerous studies were based on single-voxel techniques because they are fully automated, easy to use and do not require long acquisition time. However, they result in interpretative difficulties especially when the size of the voxel is high. Indeed, the metabolite signals can be influenced by partial volume effects (signals from outside the tumor) and the spectral analysis may be hampered by tissue heterogeneity which is a characteristic of these lesions, by necrosis, hemorrhage, intraparenchymal calcification, adjacent bone tissue, cerebral edema that can be included in the assessed voxel and cause local magnetic field inhomogeneities [108,109]. Moreover, single-voxel methods do not generally allow for quantitative comparison of tumor and normal brain tissue metabolites [110], except when two voxels, one located in the lesion and the other at a similar position in the contralateral hemisphere, are successively recorded. To overcome the limitations of the single-voxel technique, a multiple-voxel 2D ^{1}H MRSI method has been used in the more recent studies as it has several

Table 2
Values of commonly used ratios for grading brain gliomas.

Study	Number and type of tumors analyzed	tCho/tCr		tNAA/tCr		tCho/tNAA		Measurement conditions	
		HG	LG	HG	LG	HG	LG		
Zeng et al. [112]	25 HG (10 III, 15 IV) 12 LG (4 I, 8 II)	2.94 ± 1.83	1.72 ± 0.62	0.72 ± 0.35	0.89 ± 0.50	3.65 ± 3.14	1.97 ± 1.10	Multivoxel TR 1000 ms TE 144 ms	NN[a] ratios in the lesion: max tCho/tCr and tCho/tNAA, and min tNAA/tCr
Server et al. [118]	53 HG (19 AA III, 34 GBM IV)	3.91 ± 3.09 GBM 3.50 ± 2.03 AA 4.65 ± 4.38		0.86 ± 0.91 GBM 0.87 ± 0.89 AA 0.85 ± 0.98		6.97 ± 5.63 GBM 7.31 ± 6.00 AA 6.36 ± 5.00		Multivoxel TR 1500 ms TE 135 ms	NN ratios in the tumor core: max tCho/tCr and tCho/tNAA, and min tNAA/tCr
Senft et al. [111]	36 HG (26 III, 10 IV) 27 LG (II)	1.33 ± 0.30	0.40 ± 0.03					Multivoxel TR 1500 ms TE 144 ms	Absolute concentrations (phantom, T_1 and T_2 corrected) N[a] to normal tissue for tCho Max tCho in tumor
Hourani et al. [119]	28 HG 8 LG	2.84 ± 2.43	2.10 ± 0.98	0.78 ± 0.28	1.05 ± 0.51	2.94[b]	1.72[b]	Multivoxel TR 1700 or 2300 ms TE 280 ms	NN ratios in the lesion and determination of normalized tCho, tNAA and tCr to normal tissue
Toyooka et al. [120]	10 HG (5 III, 5 IV) 13 LG (II)	≈1 (III) ≈1.2 (IV)	≈0.5	≈0.8 (III and IV)	≈1.1			Single-voxel TR 2000 ms TE 136 ms	NN ratios
Spampinato et al. [121]	8 HG 12 LG Oligodendroglioma and oligoastrocytoma	4.23 ± 2.46	2.03 ± 2.05	0.84 ± 0.43	1.06 ± 1.11	2.73 ± 0.82	2.78 ± 2.00	Multivoxel TR 1000 ms TE 135 ms	NN ratios in the tumor: max tCho/tCr and tCho/tNAA, and min tNAA/tCr
Yerli et al. [122]	19 HG 6 LG	NN 3.03 ± 2.34 N 1.65 ± 0.82	NN 1.75 ± 0.29 N 1.40 ± 0.64	NN 0.37 ± 0.28 N 0.29 ± 0.23	NN 0.64 ± 0.25 N 0.58 ± 0.18			Multivoxel TR 1500 ms TE 135 ms	NN ratios in the tumor: max tCho/tCr and min tNAA/tCr and N ratios to tCr in normal tissue: max $tCho/tCr_{norm}$ and min $tNAA/tCr_{norm}$
Zonari et al. [123]	65 HG (45 III, 20 IV) 40 LG	2.47 ± 1.28 IV 2.70 ± 1.54 III 2.38 ± 1.15	2.01 ± 0.68	0.28 ± 0.42 IV 0.08 ± 0.23 III 0.37 ± 0.45	0.69 ± 0.41			Single-voxel TR 1500 ms TE 144 ms	NN ratios
Stadlbauer et al. [117]	17 HG 9 LG	0.66[c]	0.43[b]	0.87[b]	1.17[b]	0.81 ± 0.46	0.40 ± 0.16	Multivoxel TE 135 ms	Absolute concentrations (phantom, T_1 and T_2 corrected) Concentrations averaged across whole tumor
Chen et al. [124]	4 HG 17 LG astrocytoma	4.06 ± 1.21	2.76 ± 0.70	4.32 ± 1.57	2.14 ± 0.84			Multivoxel TR 1500 ms TE 144 ms	NN ratios in the tumor
Kim et al. [125]	28 HG (12 III, 16 IV) 7 LG	3.56 ± 3.10 IV 4.25 ± 3.83 III 2.64 ± 1.39	1.92 ± 0.89			7.09 ± 6.69 IV 6.31 ± 3.54 III 8.14 ± 9.52	4.57 ± 4.35	Single-voxel TR 1500 ms TE 144 ms	NN ratios Measurement of peak heights

[a] NN: non-normalized; N: normalized.
[b] Ratios not given by the authors and calculated from their data.

advantages. It provides multiple spectra of the tumor with spatial information for each voxel-related spectrum, thus revealing the spatial heterogeneity of gliomas [111]. Furthermore, additional spectra from healthy brain tissue can be acquired in the same measurement offering the opportunity to express the levels of metabolites in tumor directly in those detected in unaffected brain tissue [110]. However, the analysis is restricted to a single slice. To more accurately evaluate each part of the entire lesion and so to minimize sampling errors, one can resort to 3D ^{1}H MRSI whose advantage is an increase of spatial coverage in the three-dimensional space; it nevertheless requires longer acquisition times [112].

Major signals detected in ^{1}H MRS spectra of cerebral gliomas are those of choline-containing-compounds (tCho) encompassing at least GPC, PC and Cho, total creatine (tCr) (Cr and phosphocreatine), lipids and other macromolecules, lactate, glutamine and glutamate (Glx), myo-inositol, NAA and N-acetylaspartyl glutamate (tNAA). In most studies reported so far, two metabolites have a pivotal role in glioma grading, tCho and tNAA. HG gliomas tend to have lower tNAA intensities and higher tCho intensities than LG gliomas [113].

Data interpretation of the literature is not straightforward as the diagnosis is based on different parameters according to the authors: metabolite ratios, absolute concentrations of metabolites, mean or maximum values of metabolite concentrations in multivoxel approaches. Moreover, data can be normalized or not. As the intensity of the tCr peak remains stable or only mildly changed in tumor spectra, it is commonly considered as an internal reference and the ratios tCho/tCr and tNAA/tCr have been predominantly used to grade brain tumors. However, increased and decreased tCr levels in different brain tumors and even in different regions of the same tumor have been reported [114–116]. For example, Hattingen et al. [116] have demonstrated that the normalized to contralateral normal brain tissue value of tCr in WHO grade II gliomas is a significant predictor for tumor progression and for malignant tumor transformation. LG gliomas with decreased tCr may show longer progression-free times and later malignant transformation than LG gliomas with regular or increased tCr values. Stadlbauer et al. [117] observed a significant difference for the tCr value in the voxel showing the maximum tCr concentration within the tumor. All patients with a grade III oligoastrocytoma or oligodendroglioma had a maximum concentration <7 mmol L^{-1}, whereas those with a grade III astrocytoma had a maximum concentration >7 mmol L^{-1}.

The discrepancies of the tCho/tCr, tNAA/tCr and tCho/tNAA values shown in Table 2 may have several origins. The first one is the way of calculating metabolite ratios. Most studies reported non-normalized "standard" ratios obtained from metabolites within the lesion (e.g. $tCho_{tum}/tCr_{tum}$), even with a multivoxel approach which easily enables a ratio of one metabolite from the diagnostic voxel to another (or the same) metabolite from the contralateral hemisphere (e.g. $tCho_{tum}/tCr_{normalized}$). This implies that the contralateral tissue is truly healthy. However, Kallenberg et al. [109] have recently reported increased absolute concentrations of myo-inositol and glutamine in the contralateral normal-appearing white matter in patients with GBM that could be due to neoplastic infiltration. The concentrations of tNAA, tCr, tCho and glutamate were nevertheless not altered. There is currently no consensus in the literature on which type of differently calculated ratios is the better to be considered [110,126,127]. Yerli et al. [122] evaluated the two ways of calculating ratios: normalized ratios in which tCr from the normal contralateral hemisphere was used as denominator were compared with non-normalized ratios obtained from metabolites in the lesion (both as the numerator and the denominator) (Table 2). Whereas the standard ratio max-tCho/tCr was significantly different ($p = 0.007$) between HG and LG tumors, the normalized ratio $max\text{-}tCho/tCr_{normalized}$ did not allow discriminating HG and LG tumors ($p = 0.525$). Maybe future studies should use both types of ratios in order to improve the accuracy of the ^{1}H MRS method for grading gliomas.

In order to generate more stable measures of tCho abnormality, particularly in voxels that have low tNAA or tCr, which can drive the direct ratio to very large values irrespective of the tCho level, McKnight et al. [128,129] developed two indexes, the so called CCI (tCho-to-tCr index) and CNI (tCho-to-tNAA index). These indices, generated by a linear regression-based method, reflect the number of standard deviations of difference between the relative level of tCho in a given voxel and the mean relative level of tCho in voxels from non-tumor regions. The authors demonstrated that the best criterion for choosing an appropriate biopsy target in presumed grade II or grade III gliomas would be that both the standard tCho/tNAA ratio and the CNI are near their maximum values.

Some authors measured absolute concentrations of metabolites in order to avoid ratios which can artificially enhance or conversely reduce the differences [111,117]. For example, Stadlbauer et al. [117] measured significantly lower tCho levels (2.24 ± 0.37 mmol L^{-1} vs 3.21 ± 1.04 mmol L^{-1}, $p = 0.002$) and higher tNAA levels (6.10 ± 1.64 mmol L^{-1} vs 4.25 ± 0.99 mmol L^{-1}, $p = 0.010$) in grade II tumors compared with grade III tumors.

The highly variable values reported in Table 2 may also arise from the fact that many authors did not stratify their studies according to the nature of the glioma. Under the name of HG tumors, they often mixed anaplastic astrocytomas, GBM, anaplastic oligodendrogliomas and anaplastic oligoastrocytomas, and for LG tumors, astrocytomas, oligodendrogliomas and oligoastrocytomas. All these tumors are different in terms of evolution, chemo- and/or radiosensitivity, biologic behaviour, histologic characteristics, power of infiltration, level of necrosis. However, this can be explained by the fact that astrocytomas constitute 76% of all gliomas when oligodendrogliomas and oligoastrocytomas account for ≈7% and ≈11% of glial tumors. Moreover, GBM and anaplastic astrocytomas represent ≈54% and ≈7%, respectively [101]. From these figures, it is obvious that it is statistically easier to recruit patients with astrocytomas and mostly GBM.

Another parameter to be taken into consideration is the number of patients. Few studies recruited large patient cohorts. Moreover, in several studies, patients evaluated have had previous therapeutic (adjuvant radiation and/or chemotherapy) or diagnostic interventions, which can impair the data.

A number of exploratory studies have demonstrated that ^{1}H MRS can distinguish between HG and LG gliomas. At the present time, it is still not possible to definitively predict the histologic grade of a glioma using the ^{1}H MRS pattern alone and it does not seem that ^{1}H MRS could replace the gold standard of image-guided stereotactic biopsy. However, the work deserves to be extended on larger cohorts of more homogeneous patients, with standardized procedures of ratio calculations (or absolute concentration determination), standardized diagnostic thresholds, and more accurate comparisons (i.e. not only HG vs LG but also GBM vs anaplastic astrocytoma for instance).

In vivo MRS studies clearly showed that the intensity of the tCho peak or the tCho/tCr peak ratio is higher in HG gliomas than in LG gliomas, thus demonstrating that there is a correlation between the tCho levels and the tumor malignancy. However, the *in vivo* tCho peak at ≈3.2 ppm is a complex mixture of heavily overlapping resonances, mainly Cho, GPC and PC, but also phosphoethanolamine, glycerophosphoethanolamine, taurine, myo-inositol, betaine and β-glucose. Because of its enhanced resolution, *in vitro* NMR considerably reduces signal overlapping in this highly congested region enabling to observe resonances of the different metabolites. Some studies have focused on the profile of the choline-containing compounds (GPC, PC, Cho) in perchloric acid extracts or intact tissues of biopsies from patients with gliomas using conventional high-resolution or HR-MAS NMR, respectively (e.g. [29,130]). These

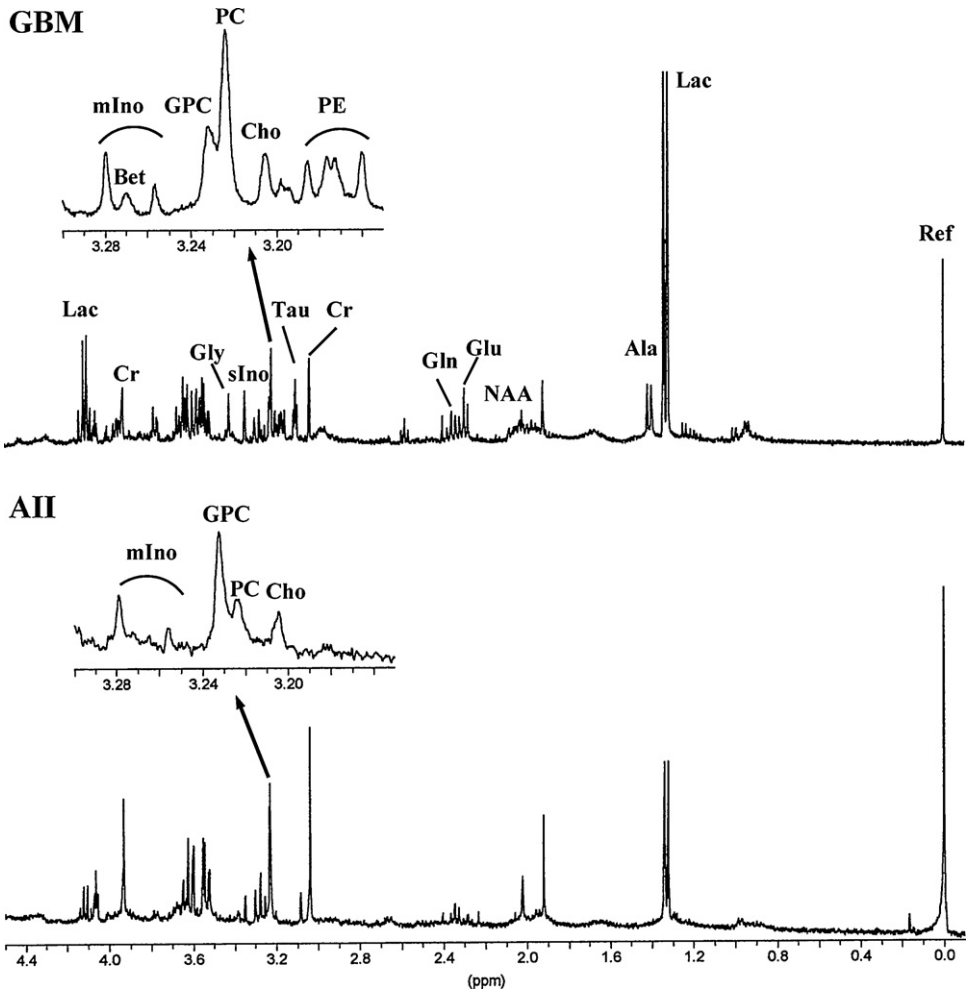

Fig. 2. ^{1}H NMR spectra of a biopsy extract of a GBM (astrocytoma grade IV, HG tumor) and an astrocytoma of grade II (AII, LG tumor). The expanded areas above the spectra show the switch in the percentages of GPC and PC. Ref: reference used for quantification; Lac: lactate; Ala: alanine; Glu: glutamate; Gln: glutamine; Tau: taurine; PE: phosphoethanolamine; Bet: betaine; mIno, myo-inositol; sIno, scyllo-inositol; Gly: glycine.

studies showed that the metabolic repartition of GPC and PC is different in HG and LG gliomas with a higher contribution of PC in HG while the GPC peak dominates in LG tumors (Fig. 2). Indeed, relative percentages of GPC and PC exhibit a crossover as they range from 69/31 to 37/63 in extracts (or 64/36 to 26/74 in intact tissues) in LG and HG gliomas, respectively. This allows to easily and accurately discriminating HG from LG gliomas. The assay of the expression of the genes involved in the Kennedy pathway (phosphatidylcholine (PtdCho) cycle) permits to understand the pattern of choline metabolites as detected by NMR. The high level of PC in HG gliomas can be explained by an upregulation of both the choline kinase β gene leading to an increase in PC synthesis, and the phospholipase C gene triggering an increased degradation of PtdCho into PC. On the other hand, the GPC accumulation in LG gliomas is supported mainly by the upregulation of phospholipase A1 and the down-regulation of phospholipase C genes [29].

A very recent HR-MAS NMR study on biopsy samples proposes to use glycine as a biomarker to distinguish several types of brain tumors, among them LG and HG gliomas. Indeed, the glycine mean concentration is higher in HG gliomas (GBM) than in LG ones, but with a limited statistical significance ($p = 0.05$) [131].

A metabolomic study of biopsies from brain tumors histologically classified as LG and HG oligodendrogliomas (LGO and HGO) was performed using HR-MAS NMR. The results of the multivariate statistical analysis show a clear separation between LGO and HGO on the basis of the whole set of metabolic variables. The distinction between HGO and LGO is principally due to the metabolites involved in the amino acid metabolism. In HGO, the production of alanine and valine, which are related to the anaerobic pathway, is increased while that of amino acids related to the Krebs pathway (proline, glutamate, glutamine, γ-aminobutyric acid and NAA) is decreased. This metabolic shift toward fermentative metabolism clearly reflects tumor hypoxia in HGO [132].

NMR is prone to the same sampling errors as histopathology because it analyzes a tiny part of the tumor. However, it can be complementary especially for cases difficult to grade with histological examination. An example of discordance between diagnoses from histology and ^{1}H NMR of biopsy extracts has been reported in two patients whose clinical evolution was in agreement with the NMR data [133]. In the future, *in vivo* MRI and MRS and *in vitro* NMR studies associated to the gold standard method should be conducted simultaneously in a multidisciplinary approach to increase confidence in tumor grading assessment.

5.2. NMR applications in pharmaceutical analysis

NMR spectroscopy can be used in pharmaceutical analysis for a couple of applications, i.e. the quality control of both active pharmaceutical ingredients (APIs) and excipients for identification, impurity assessment and assay purposes as well as determination of the origin (production plant) of the drug [134]. Similarly, drug formulations can be evaluated. Additionally, the method can be

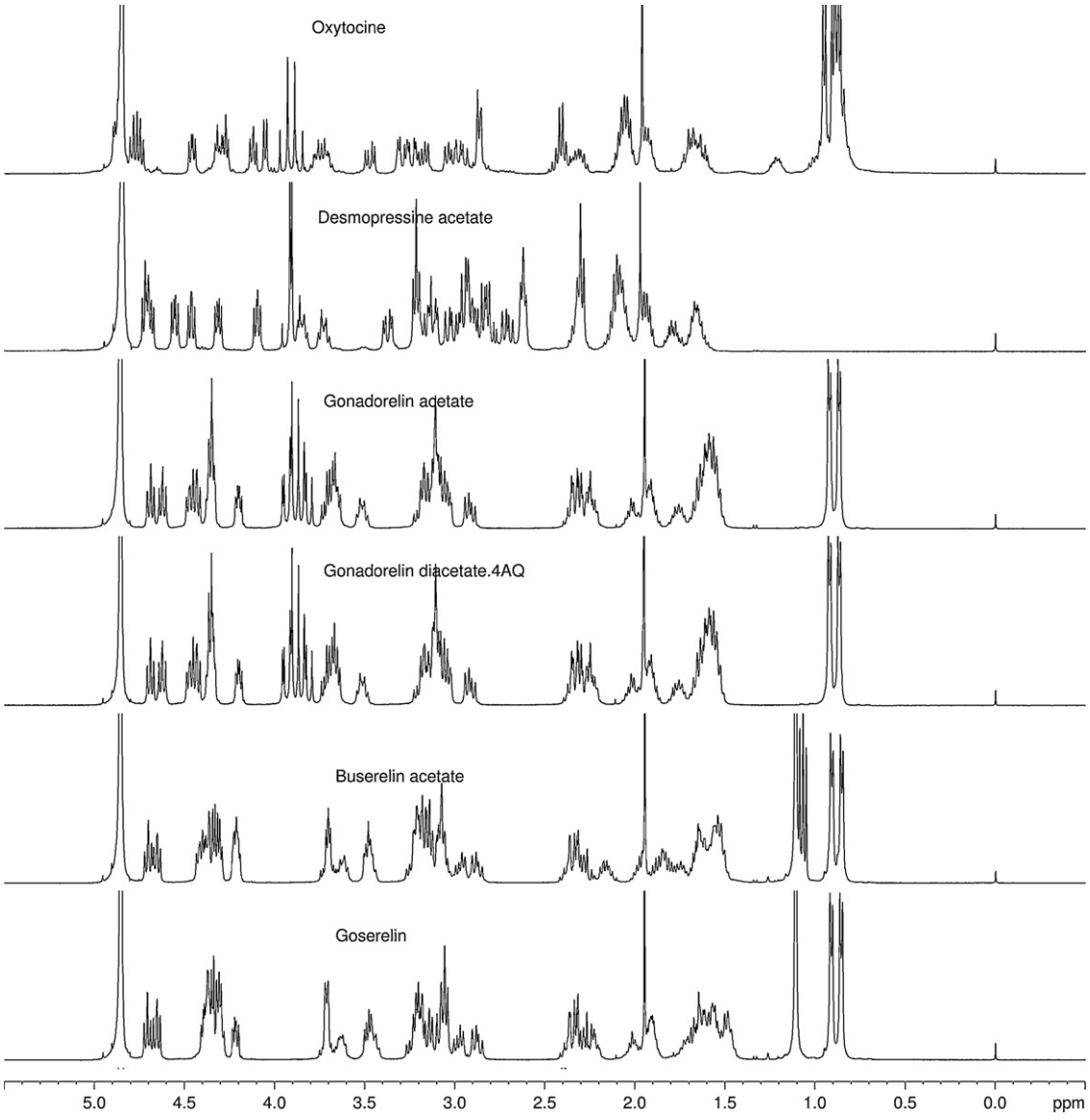

Fig. 3. 400 MHz ^{1}H NMR spectra of peptide hormones.

Modified from [139].

employed in a non-destructive manner by means of solid state NMR of formulated drugs to analyze polymorphism and imaging techniques of tablets [135].

Since ^{1}H NMR can "detect" all proton bearing molecules, it can be regarded as an universal detector and is thus highly appropriate in unraveling counterfeit drugs (see U. Holzgrabe, M. Malet-Martino, Analytical challenges in drug counterfeiting and falsification, in this issue). When it comes to the quantification of a mixture of compounds, e.g. API and excipient, components of an API, mixtures of APIs, components of an excipient, etc., NMR spectroscopy can be advantageous because (i) the quantification of all components can be performed in one run when well separated signals of all components can be found, (ii) no response factor has to be determined beforehand, and (iii) NMR spectroscopy is highly specific. The same holds true for ^{31}P NMR spectroscopy, e.g. for the characterization of the distribution and quantification of phospholipids in lipids and further fatty acid analysis [136]. Nevertheless, it is currently rarely used in quality analysis of API and drug formulations. In the following we want to demonstrate the power of NMR spectroscopy on three examples, purity control of amino acids, identity control of small peptides, and quality control of heparin derivatives.

5.2.1. Purity control of amino acids

Currently, the European Pharmacopoeia, regulating the quality control of drugs, is in the process of the revision of the impurity control of amino acids by replacing the thin layer chromatography method including the ninhydrin derivatization with a HPLC method, i.e. the amino acid analysis [137]. This method is tedious, often not robust and labor intensive. Additionally, only amino acids can be detected because all other impurities would not give a reaction with ninhydrin and thus are not found by the UV/vis detector. However, the quality of amino acids is a challenge due to the fact that most of them do not contain a chromophor, fluorophor or electrophor. Thus, they cannot be seen by the typical HPLC detectors. Beside employing HPLC in hyphenation with an evaporative light-scattering detector (ELSD), a Corona-charged aerosol detector (CAD), a nano quantity analyte detector (NQAD), or a mass detector, the impurities of alanine, i.e. malic acid, fumaric acid, aspartic acid, and glutamic acid, were recently assessed by ^{1}H NMR spectroscopy with 400 and 600 MHz NMR spectrometers using 128 and 16 scans, respectively. The limits of detection for all impurities were in the same range than the NQAD and CAD, i.e. 0.02–0.04% of the main component alanine, and even better than with the ELSD.

Only the mass detector was able to provide more sensitivity [138]. These findings clearly demonstrate that the often cited low sensitivity of the NMR spectroscopy is mostly not a problem in quality assessment.

5.2.2. Identity control of small peptides

The amino acid analysis has to be applied also for the characterization of peptide hormones and their derivatives for identifying and quantifying the amino acids [137]. However, Kellenbach et al. [139] showed that simple 1D ^{1}H NMR spectroscopy can be used to identify peptides of up to 25 amino acids, such as gonadotropin releasing hormone, its analogues, and other peptide hormones (Fig. 3). Here, NMR spectroscopy is used like IR spectroscopy as a pattern recognition method which does not need the interpretation of the spectrum but a chemical reference substance for comparison. Correspondingly NMR spectroscopy can be applied to check the batch-to-batch conformity. Even human, porcine and bovine insulin, consisting of 51 amino acids and differing in only 4, can be distinguished by their NMR spectra [140]. Furthermore, NMR spectroscopy has become a routine technology for protein characterization, not only for small proteins such as enzymes but also for large proteins like G protein-coupled receptors (for review see [141]).

5.2.3. Quality control of heparin derivatives

In 2007 and 2008, some one hundred people died from heparin contaminated with oversulfated chondroitin sulfate (OSCS) (for review see U. Holzgrabe, M. Malet-Martino, Analytical challenges in drug counterfeiting and falsification, in this issue; [134]). The heparin case happened because the monographs in the international pharmacopoeias, e.g. European Pharmacopoeia and the United States Pharmacopoeia, on unfractionated heparin were not revised for a long period and contained biological methods for identification and quality control, only. The fact that ^{1}H NMR spectroscopy was able to identify OSCS [142] and to guarantee the absence of impurities related to heparin in addition to residual solvents [143,144] created a NMR hype worldwide resulting in dozens of NMR papers. The most recent ones are dealing with the identification, characterization and quantification of old and new heparin impurities often using multivariate analysis [145–149] and monitoring the production process [150].

Especially the heparin case leaves the hope that NMR spectroscopy will be applied in quality analysis of APIs and excipients more often in the future in order to avoid substandard drugs appearing on the market on the one hand. On the other hand, NMR spectroscopy can be a powerful alternative when the classical HPLC-UV or HPLC-fluorescence analysis is not possible.

6. Conclusion

This article has described the various abilities of NMR spectroscopy in the field of biomedical and pharmaceutical research. Mostly used at its beginning by chemists as a tool for structural elucidation, it has spread to Biochemistry, Pharmacy and Medicine among other disciplines. This is due to its unique properties that are largely discussed here. The versatility of NMR has enabled the technique to make significant and valuable contributions to both the *in vitro* analysis of complex mixtures as drugs, biofluids, intact tissue samples and the *in vivo* clinical investigations. *In vitro* NMR is a well established analytical technique even if in our opinion its true merit is not sufficiently recognized. MRI has proven to be essential for clinicians in diagnosis and monitoring of pathology. However, despite promising data, *in vivo* MRS has still to demonstrate its additional diagnostic value before being routinely included in the clinical practice. With the present technological developments and the establishment of larger and more organized studies, the benefit of MRS should be demonstrated in the near future.

References

[1] E.M. Purcell, H.C. Torrey, R.V. Pound, Resonance absorption by nuclear magnetic moments in a solid, Phys. Rev. 69 (1946) 37–38.
[2] F. Bloch, W.W. Hansen, M. Packard, Nuclear induction, Phys. Rev. 69 (1946) 127.
[3] F. Bloch, W.W. Hansen, M. Packard, The nuclear induction experiment, Phys. Rev. 70 (1946) 474–485.
[4] M.J. Avison, H.P. Hetherington, R.G. Shulman, Application of NMR to studies of tissue metabolism, Annu. Rev. Biophys. Biophys. Chem. 15 (1986) 377–402.
[5] S. Cabanac, M.C. Malet-Martino, M. Bon, R. Martino, J.F. Nedelec, J.L. Dimicoli, Direct ^{19}F NMR spectroscopic observation of 5-fluorouracil metabolism in the isolated perfused mouse liver model, NMR Biomed. 1 (1988) 113–120.
[6] J.K. Nicholson, I.D. Wilson, High resolution proton magnetic resonance spectroscopy of biological fluids, Prog. NMR Spectrosc. 21 (1989) 449–501.
[7] M.C. Malet-Martino, R. Martino, Magnetic resonance spectroscopy: a powerful tool for drug metabolism studies, Biochimie 74 (1992) 785–800.
[8] G.F. King, P.W. Kuchel, Theoretical and practical aspects of NMR studies of cells, Immunomethods 4 (1994) 85–97.
[9] J.C. Lindon, J.K. Nicholson, J.R. Everett, NMR spectroscopy of biofluids, in: G.A. Webb (Ed.), Annual Reports on NMR Spectroscopy, vol. 38, Academic Press, London, 1999, pp. 1–88.
[10] N. Ogrinc, I.G. Kosir, J.E. Spangenberg, J. Kidric, The application of NMR and MS methods for detection of adulteration of wine, fruit juices and olive oil. A review, Anal. Bioanal. Chem. 376 (2003) 424–430.
[11] R. Martino, V. Gilard, F. Desmoulin, M. Malet-Martino, Fluorine-19 or phosphorus-31 NMR spectroscopy: a suitable analytical technique for quantitative in vitro metabolic studies of fluorinated or phosphorylated drugs, J. Pharm. Biomed. Anal. 38 (2005) 871–891.
[12] U. Holzgrabe, Quantitative NMR spectroscopy in pharmaceutical applications, Progr. NMR Spectrosc. 57 (2010) 229–240.
[13] O. Beckonert, M. Coen, H.C. Keun, Y. Wang, T.M.D. Ebbels, E. Holmes, J.C. Lindon, J.K. Nicholson, High-resolution magic-angle-spinning NMR spectroscopy for metabolic profiling of intact tissues, Nat. Protoc. 5 (2010) 1019–1032.
[14] O. Robert, J. Sabatier, D. Desoubzdanne, J. Lalande, S. Balayssac, V. Gilard, R. Martino, M. Malet-Martino, pH optimization for a reliable quantification of brain tumor cell and tissue extracts with ^{1}H NMR: focus on choline-containing compounds and taurine, Anal. Bioanal. Chem. 399 (2011) 987–999.
[15] V. Gilard, S. Balayssac, M. Malet-Martino, R. Martino, Quality control of herbal medicines assessed by NMR, Curr. Pharm. Anal. 6 (2010) 234–245.
[16] O. Henriksen, MR spectroscopy in clinical research, Acta Radiol. 35 (1994) 96–116.
[17] R. Bligny, R. Dousse, NMR and plant metabolism, Curr. Opin. Plant Biol. 4 (2001) 191–196.
[18] I.M. Burtscher, S. Holtas, Proton MR spectroscopy in clinical routine, J. Magn. Reson. Imaging 13 (2001) 560–567.
[19] A.R. Neves, W.A. Pool, J. Kok, O.P. Kuipers, H. Santos, Overview on sugar metabolism and its control in Lactococcus lactis – the input from in vivo NMR, FEMS Microbiol. Rev. 29 (2005) 531–554.
[20] D. Lee, D. Marcinek, Noninvasive in vivo small animal MRI and MRS: basic experimental procedures, J. Vis. Exp. 32 (2009) 1592.
[21] E.M. Ratai, S. Pilkenton, M.R. Lentz, J.B. Greco, R.A. Fuller, J.P. Kim, J. He, L.L. Cheng, R.G. Gonzalez, Comparisons of brain metabolites observed by HRMAS ^{1}H NMR of intact tissues and solution ^{1}H NMR of tissue extracts in SIV-infected macaques, NMR Biomed. 18 (2005) 242–251.
[22] W.E. Hull, Measurement of absolute metabolite concentrations in biological samples, Bruker Rep. 2 (1986) 15–19.
[23] F. Malz, Quantitative NMR in the solution state NMR, in: U. Holzgrabe, I. Wawer, B. Diehl (Eds.), NMR Spectroscopy in Pharmaceutical Analysis, Elsevier, Amsterdam, 2008, pp. 43–62.
[24] C.K. Larive, D. Jayawickrama, L. Orfi, Quantitative analysis of peptides with NMR spectroscopy, Appl. Spectrosc. 51 (1997) 1531–1536.
[25] L. Griffiths, A.M. Irving, Assay by nuclear magnetic resonance spectroscopy: quantification limits, Analyst 123 (1998) 1061–1068.
[26] G.F. Pauli, B.U. Jaki, D.C. Lankin, Quantitative ^{1}H NMR: development and potential of a method for natural products analysis, J. Nat. Prod. 68 (2005) 133–149.
[27] T. Beyer, C. Schollmayer, U. Holzgrabe, The role of solvents in the signal separation for quantitative ^{1}H NMR spectroscopy, J. Pharm. Biomed. Anal. 52 (2010) 51–58.
[28] G. Reynolds, M. Wilson, A. Peet, T.N. Arvanitis, An algorithm for the automated quantitation of metabolites in in vitro NMR signals, Magn. Reson. Med. 56 (2006) 1211–1219.
[29] V. Righi, J.M. Roda, J. Paz, A. Mucci, V. Tugnoli, G. Rodriguez-Tarduchy, L. Barrios, L. Schenetti, S. Cerdan, M.L. Garcia-Martin, ^{1}H HR-MAS and genomic analysis of human tumor biopsies discriminate between high and low grade astrocytomas, NMR Biomed. 22 (2009) 629–637.
[30] E.Y. Xu, W.H. Schaefer, Q. Xu, Metabolomics in pharmaceutical research and development: metabolites, mechanisms and pathways, Curr. Opin. Drug Discov. Dev. 12 (2009) 40–52, and references quoted in.

[31] B. Sitter, S. Lundgren, T.F. Bathen, J. Halgunset, H.E. Fjosne, I.S. Gribbestad, Comparison of HR MAS MR spectroscopic profiles of breast cancer tissue with clinical parameters, NMR Biomed. 19 (2006) 30–40.
[32] D. Morvan, A. Demidem, J. Papon, M. De Latour, J.C. Madelmont, Melanoma tumors acquire a new phospholipid metabolism phenotype under cystemustine as revealed by High-Resolution Magic Angle Spinning Proton Nuclear Magnetic Resonance spectroscopy of intact tumor samples, Cancer Res. 62 (2002) 1890–1897.
[33] M.G. Swanson, K.R. Keshari, Z.L. Tabatabai, J.P. Simko, K. Shinohara, P.R. Carroll, A.S. Zektzer, J. Kurhanewicz, Quantification of choline- and ethanolamine-containing metabolites in human prostate tissues using ^{1}H HR-MAS total correlation spectroscopy, Magn. Reson. Med. 60 (2008) 33–40.
[34] O.C. Andronesi, K.D. Blekas, D. Mintzopoulos, L. Astrakas, P.M. Black, A.A. Tzika, Molecular classification of brain tumor biopsies using solid-state magic angle spinning proton magnetic resonance spectroscopy and robust classifiers, Int. J. Oncol. 33 (2008) 1017–1025.
[35] M. Bayet-Robert, D. Loiseau, P. Rio, A. Demidem, C. Barthomeuf, G. Stepien, D. Morvan, Quantitative two-dimensional HRMAS ^{1}H-NMR spectroscopy-based metabolite profiling of human cancer cell lines and response to chemotherapy, Magn. Reson. Med. 63 (2010) 1172–1183.
[36] S. Tiziani, A.-H. Emwas, A. Lodi, C. Ludwig, C.M. Bunce, M.R. Viant, U.L. Günther, Optimized metabolite extraction from blood serum for ^{1}H nuclear magnetic resonance spectroscopy, Anal. Biochem. 377 (2008) 16–23.
[37] N.J. Serkova, K. Glunde, Metabolomics of cancer, Methods Mol. Biol. Tumor Biomark. Discov. 520 (2009) 273–295.
[38] A.A. Tzika, L. Astrakas, H. Cao, D. Mintzopoulos, O. Andronesi, M. Mindrinos, J. Zhang, L.G. Rahme, K.D. Blekas, A.C. Likas, N.P. Galatsanos, R.S. Carroll, P.M. Black, Combination of high-resolution magic angle spinning proton magnetic resonance spectroscopy and microscale genomics to type brain tumor biopsies, Int. J. Mol. Med. 20 (2007) 199–208.
[39] M.B. Tessem, M.G. Swanson, K.R. Keshari, M.J. Albers, D. Joun, Z.L. Tabatabai, J.P. Simko, K. Shinohara, S.J. Nelson, D.B. Vigneron, I.S. Gribbestad, J. Kurhanewicz, Evaluation of lactate and alanine as metabolic biomarkers of prostate cancer using ^{1}H HR-MAS spectroscopy of biopsy tissues, Magn. Reson. Med. 60 (2008) 510–516.
[40] M.C. Martínez-Bisbal, D. Monleon, O. Assemat, M. Piotto, J. Piquer, J.L. Llácer, B. Celda, Determination of metabolite concentrations in human brain tumour biopsy samples using HR-MAS and ERETIC measurements, NMR Biomed. 22 (2009) 199–206.
[41] M.J. Albers, T.N. Butler, I. Rahwa, N. Bao, K.R. Keshari, M.G. Swanson, J. Kurhanewicz, Evaluation of the ERETIC method as an improved quantitative reference for ^{1}H HR-MAS spectroscopy of prostate tissue, Magn. Res. Med. 61 (2009) 525–532.
[42] B. Sitter, T.F. Bathen, T.E. Singstad, H.E. Fjosne, S. Lundgren, J. Halgunset, I.S. Gribbestad, Quantification of metabolites in breast cancer patients with different clinical prognosis using HR MAS MR spectroscopy, NMR Biomed. 23 (2010) 424–431.
[43] A.G. Webb, Microcoil Nuclear Magnetic Resonance spectroscopy, in: U. Holzgrabe, I. Wawer, B. Diehl (Eds.), NMR Spectroscopy in Pharmaceutical Analysis, Elsevier, Amsterdam, 2008, pp. 83–130.
[44] R.A. Wevers, U.D.F. Engelke, S.H. Moolenaar, C. Brautigam, J.G.N. de Jong, R. Duran, R.A. de Abreu, A.H. van Gennip, ^{1}H-NMR spectroscopy of body fluids: inborn errors of purine and pyrimidine metabolism, Clin. Chem. 45 (1999) 539–548.
[45] S.H. Moolenaar, G. Gohlich-Ratmann, U.F.H. Engelke, M. Spraul, E. Humpfer, P. Dvortsak, T. Voit, G.H. Hoffmann, C. Brautigam, A.B. van Kuilenburg, A. van Gennip, P. Vreken, R.A. Wevers, β-Ureidopropionase deficiency: a novel inborn error of metabolism discovered using NMR spectroscopy on urine, Magn. Reson. Med. 46 (2001) 1014–1017.
[46] G. Schlotterbeck, A. Ross, R. Hochstrasser, H. Senn, T. Kühn, D. Marek, O. Schett, High-resolution capillary tube NMR. A miniaturized 5-μL high-sensitivity TXI probe for mass-limited samples, off-line LC NMR, and HT NMR, Anal. Chem. 74 (2002) 4464–4471.
[47] D.L. Olson, J.A. Norcross, M. O'Neil-Johnson, P.F. Molitor, D.J. Detlefsen, A.G. Wilson, T.L. Peck, Microflow NMR: concepts and capabilities, Anal. Chem. 76 (2004) 2966–2974.
[48] TCI 1.7 mm Microcryoprobe™-New heights in NMR sensitivity, 2010. www.bruker.biospin.com/cryoprobe_micro.html.
[49] J.K. Nicholson, J.C. Lindon, E. Holmes, "Metabonomics": understanding the metabolic responses of living systems to pathophysiological stimuli via multivariate statistical analysis of biological NMR spectroscopic data, Xenobiotica 29 (1999) 1181–1189.
[50] M. Coen, E. Holmes, J.C. Lindon, J.K. Nicholson, NMR-based metabolic profiling and metabonomic approaches to problems in molecular toxicology, Chem. Res. Toxicol. 21 (2008) 9–27.
[51] O. Beckonert, H.C. Keun, T.M.D. Ebbels, J. Bundy, E. Holmes, J.C. Lindon, J.K. Nicholson, Metabolic profiling, metabolomic and metabonomic procedures for NMR spectroscopy of urine, plasma, serum and tissue extracts, Nat. Protoc. 2 (2007) 2692–2703.
[52] C.Y Lin, H. Wu, R.S. Tjeerdema, M.R. Viant, Evaluation of metabolite extraction strategies from tissue samples using NMR metabolomics, Metabolomics 3 (2007) 55–67.
[53] H. Wu, A.D. Southam, A. Hines, M.R. Viant, High-throughput tissue extraction protocol for NMR- and MS-based metabolomics, Anal. Biochem. 372 (2008) 204–212.
[54] H.J. Issaq, Q.N. Van, T.J. Waybright, G.M. Muschik, T.D. Veenstra, Analytical and statistical approaches to metabolomics research, J. Sep. Sci. 32 (2009) 2183–2199.
[55] A. Craig, O. Cloarec, E. Holmes, J.K. Nicholson, J.C. Lindon, Scaling and normalization effects in NMR spectroscopic metabonomic data sets, Anal. Chem. 78 (2006) 2262–2267.
[56] S. Zhang, C. Zheng, I.R. Lanza, K.S. Nair, D. Raftery, O. Vitek, Interdependence of signal processing and analysis of urine ^{1}H NMR spectra for metabolic profiling, Anal. Chem. 81 (2009) 6080–6088.
[57] T. De Meyer, D. Sinnaeve, B. Van Gasse, E.-R. Rietzschel, M.L. De Buyzere, M.R. Langlois, S. Bekaert, J.C. Martins, W. Van Criekinge, Evaluation of standard and advanced preprocessing methods for the univariate analysis of blood serum ^{1}H-NMR spectra, Anal. Bioanal. Chem. 398 (2010) 1781–1790.
[58] F. Dieterle, A. Ross, G. Schlotterbeck, H. Senn, Probabilistic quotient normalization as robust method to account for dilution of complex biological mixtures. Application in ^{1}H NMR metabonomics, Anal. Chem. 78 (2006) 4281–4290.
[59] R.J.O. Torgrip, K.M. Aberg, E. Alm, I. Schuppe-Koistinen, J. Lindberg, A note on normalization of biofluid 1D ^{1}H-NMR data, Metabolomics 4 (2008) 114–121.
[60] R.A. van den Berg, H.C.J. Hoefsloot, J.A. Westerhuis, A.K. Smilde, M.J. van der Werf, Centering, scaling, and transformations: improving the biological information content of metabolomics data, BMC Genom. 7 (2006) 142.
[61] J Trygg, E. Holmes, T. Lundstedt, Chemometrics in metabonomics, J. Proteome Res. 6 (2007) 469–479.
[62] Human Metabolome Database, Version 2.5, 2009. www.hmdb.ca.
[63] Madison Quingdao Metabolomics Consortium Database, 2008. www.mmcd.nmrfam.wisc.edu.
[64] Biological Magnetic Resonance Data Bank, 2010. www.bmrb.wisc.edu.
[65] The Magnetic Resonance Metabolomics Database, 2005. www.liu.se/hu/mdl/main.
[66] Chenomx NMR Suite 7.0, 2010. www.chenomx.com/services.
[67] AMIX: Exploring of Spectroscopic Data, 2010. www.bruker-biospin.com/amix.
[68] J. Xia, T.C. Bjorndahl, P. Tang, D.S. Wishart, MetaboMiner-semi-automated identification of metabolites from 2D NMR spectra of complex biofluids, BMC Bioinform. 9 (2008) 507, www.wishart.biology.ualberta.ca/metabominer/.
[69] I.A. Lewis, S.C. Schommer, J.L. Markley, rNMR: open source software for identifying and quantifying metabolites in NMR spectra, Magn. Reson. Chem. 47 (2009) S123–S126, www.rnmr.nmrfam.wisc.edu.
[70] O Cloarec, M. -E. Dumas, A. Craig, R.H. Barton, J. Trygg, J. Hudson, C. Blancher, D. Gauguier, J.C. Lindon, E. Holmes, J. Nicholson, Statistical Total Correlation Spectroscopy: an exploratory approach for latent biomarker identification from metabolic ^{1}H NMR data sets, Anal. Chem. 77 (2005) 1282–1289.
[71] J.C. Lindon, J.K. Nicholson, Analytical technologies for metabonomics and metabolomics, and multi-omic information recovery, Trends Anal. Chem. 27 (2008) 194–204.
[72] J.L. Spratlin, N.J. Serkova, S.G. Eckhardt, Clinical applications of metabolomics in oncology: a review, Clin. Cancer Res. 15 (2009) 431–440.
[73] E. Moser, Ultra-high-field magnetic resonance: why and when? World J. Radiol. 2 (2010) 37–40.
[74] P.B. Barker, D.O. Hearshen, M.D. Boska, Single-voxel proton MRS of the human brain at 1.5 T and 3.0 T, Magn. Reson. Med. 45 (2001) 765–769.
[75] P.B. Barker, D.D.M. Lin, In vivo proton MR spectroscopy of the human brain, Progr. NMR Spectrosc. 49 (2006) 99–128.
[76] T.E. Sjøbakk, S. Lundgren, A. Kristoffersen, T. Singstad, A.J. Svarliaunet, U. Sonnewald, I.S. Gribbestad, Clinical ^{1}H Magnetic Resonance Spectroscopy of brain metastases at 1.5 T and 3 T, Acta Radiol. 47 (2006) 501–508.
[77] I. Tkac, G. Oz, G. Adriany, K. Ugurbil, R. Gruetter, In vivo ^{1}H NMR spectroscopy of the human brain at high magnetic fields: metabolite quantification at 4 T vs. 7 T, Magn. Reson. Med. 62 (2009) 868–879.
[78] A. Haase, J. Frahm, W. Hanicke, D. Matthaei, ^{1}H NMR chemical shift selective (CHESS) imaging, Phys. Med. Biol. 30 (1985) 341–344.
[79] R.J. Ogg, R.B. Kingsley, J.S. Taylor, WET, a T_1- and B_1-insensitive water-suppression method for *in vivo* localized ^{1}H NMR spectroscopy, J. Magn. Reson. B 104 (1994) 1–10.
[80] M. Mescher, H. Merkle, J. Kirsch, M. Garwood, R. Gruetter, Simultaneous in vivo spectral editing and water suppression, NMR Biomed. 11 (1998) 266–272.
[81] J. Star-Lack, D.B. Vigneron, J. Pauly, J. Kurhanewicz, S.J. Nelson, Improved solvent suppression and increased spatial excitation bandwidths for three dimensional PRESS CSI using phase-compensating spectral/spatial spin–echo pulses, J. Magn. Reson. Imaging 7 (1997) 745–757.
[82] R.G. Males, D.B. Vigneron, J. Star-Lack, S.C. Falbo, S.J. Nelson, H. Hricak, J. Kurhanewicz, Clinical application of BASING and spectral/spatial water and lipid suppression pulses for prostate cancer staging and localization by in vivo 3D ^{1}H Magnetic Resonance Spectroscopic Imaging, Magn. Reson. Med. 43 (2000) 17–22.
[83] P. Stanwell, C. Mountford, In vivo proton MR spectroscopy of the breast, RadioGraphics 27 (2007) S253–S266.
[84] T.R. Brown, B.M. Kincaid, K. Ugurbil, NMR Chemical Shift Imaging in three dimensions, Proc. Natl. Acad. Sci. U.S.A. 79 (1982) 3523–3526.
[85] A. Skoch, F. Jiru, J. Bunke, Spectroscopic imaging: basic principles, Eur. J. Radiol. 67 (2008) 230–239.
[86] M. van der Graaf, In vivo magnetic resonance spectroscopy: basic methodology and clinical applications, Eur. Biophys. J. 39 (2010) 527–540.

[87] P.A. Bottomley, Spatial localization in NMR-spectroscopy in vivo, Ann. N. Y. Acad. Sci. 508 (1987) 333–348.
[88] J. Frahm, H. Bruhn, M.L. Gyngell, K.D. Merboldt, W. Hanicke, R. Sauter, Localized high-resolution proton NMR spectroscopy using stimulated echoes: initial applications to human brain in vivo, Magn. Reson. Med. 9 (1989) 79–93.
[89] M. Henneke, S. Dreha-Kulaczewski, K. Brockmann, M. van der Graaf, M.A.A.P. Willemsen, U. Engelke, P. Dechent, A. Heerschap, G. Helms, R.A. Wevers, J. Gärtner, *In vivo* proton MR spectroscopy findings specific for adenylosuccinate lyase deficiency, NMR Biomed. 23 (2010) 441–445.
[90] C. Choi, I.E. Dimitrov, D. Douglas, A. Patel, L.G. Kaiser, C.A. Amezcua, E.A. Maher, Improvement of resolution for brain coupled metabolites by optimized ^{1}H MRS at 7 T, NMR Biomed. 23 (2010) 1044–1052.
[91] V. Govindaraju, K. Young, A.A. Maudsley, Proton NMR chemical shifts and coupling constants for brain metabolites, NMR Biomed. 13 (2000) 129–153.
[92] M. Terpstra, K. Ugurbil, I. Tkac, Noninvasive quantification of human brain ascorbate concentration using ^{1}H NMR spectroscopy at 7 T, NMR Biomed. 23 (2010) 227–232.
[93] M.A. Thomas, S. Lipnick, S.S. Velan, X. Liu, S. Banakar, N. Binesh, S. Ramadan, A. Ambrosio, R.R. Raylman, J. Sayre, N. DeBruhl, L. Bassett, Investigation of breast cancer using two-dimensional MRS, NMR Biomed. 22 (2009) 77–91.
[94] J.F.A. Jansen, W.H. Backes, K. Nicolay, M.E. Kooi, ^{1}H MR spectroscopy of the brain: absolute quantification of metabolites, Radiology 240 (2006) 318–332, and references quoted in.
[95] S.W. Provencher, Estimation of metabolite concentrations from localized in vivo proton NMR spectra, Magn. Reson. Med. 30 (1993) 672–679, http://s-provencher.com/pages/lcmodel.shtml.
[96] A. Naressi, C. Couturier, J.M. Devos, M. Janssen, C. Mangeat, R. de Beer, D. Graveron-Demilly, Magn. Reson. Mater. Phys. 12 (2001) 141–152, http://www.mrui.uab.es/mrui/.
[97] G. Grasso, C. Alafaci, M. Passalacqua, A. Morabito, M. Buemi, F. Salpietro, F. Tomasello, Assessment of human brain water content by cerebral bioelectrical impedance analysis: a new technique and its application to cerebral pathological conditions, Neurosurgery 50 (2002) 1064–1072.
[98] S. Heinzer-Schweizer, N. De Zanche, M. Pavan, G. Mens, U. Sturzenegger, A. Henning, P. Boesiger, *In-vivo* assessment of tissue metabolite levels using ^{1}H MRS and the Electric REference To access *In vivo* Concentrations (ERETIC) method, NMR Biomed. 23 (2010) 406–413.
[99] D.P. Soares, M. Law, Magnetic resonance spectroscopy of the brain: review of metabolites and clinical applications, Clin. Radiol. 64 (2009) 12–21.
[100] E.M. DeFeo, L.L. Cheng, Characterizing human cancer metabolomics with *ex vivo* ^{1}H HRMAS MRS, Technol. Cancer Res. Treatment 9 (2010) 381–391.
[101] CBTRUS, CBTRUS Statistical Report: Primary Brain and Central Nervous System Tumors Diagnosed in the United States in 2004–2006, Central Brain Tumor Registry of the United States, Hinsdale, IL, 2010, http://www.cbtrus.org/reports/.
[102] Brain Tumor – Primary-adults, MedlinePlus Medical Encyclopedia, 2009. www.nlm.nih.gov/medlineplus/.
[103] D.N. Louis, H. Ohgaki, O.D. Wiestler, W.K. Cavenee, P.C. Burger, A. Jouvet, B.W. Scheithauer, P. Kleihues, The 2007 WHO classification of tumours of the central nervous system, Acta Neuropathol. 114 (2007) 97–109.
[104] M.L. Apuzzo, P.T. Chandrasoma, D. Cohen, C.S. Zee, V. Zelman, Computed image stereotaxy: experience and perspective related to 500 procedures applied to brain masses, Neurosurgery 20 (1987) 930–937.
[105] M.A. Mittler, B.C. Walters, E.G. Stopa, Observer reliability in histological grading of astrocytoma stereotactic biopsies, J. Neurosurg. 85 (1996) 1091–1094.
[106] D. Trembath, C.R. Miller, A. Perry, Gray zones in brain tumor classification: evolving concepts, Adv. Anat. Pathol. 15 (2008) 287–297.
[107] W. Hollingworth, L.S. Medina, R.E. Lenkinski, D.K. Shibata, B. Bernal, D. Zurakowski, B. Cormstock, J.G. Jarvik, A systematic literature review of magnetic resonance spectroscopy for the characterization of brain tumors, AJNR Am. J. Neuroradiol. 27 (2006) 1404–1411.
[108] M. Setzer, S. Herminghaus, G. Marquardt, D.S. Tews, U. Pilatus, V. Seifert, F. Zanella, H. Lanfermann, Diagnostic impact of proton MR-spectroscopy versus image-guided stereotactic biopsy, Acta Neurochir. 149 (2007) 379–386.
[109] K. Kallenberg, H.C. Bock, G. Helms, K. Jung, A. Wrede, J.-H. Buhk, A. Giese, J. Frahm, H. Strik, P. Dechent, M. Knauth, Untreated glioblastoma multiforme: increased *myo*-inositol and glutamine levels in the contralateral cerebral hemisphere at proton MR spectroscopy, Radiology 253 (2009) 805–812.
[110] P.E. Sijens, Response to article "Proton magnetic resonance spectroscopy in the distinction of high-grade cerebral gliomas from single metastatic brain tumors", Acta Radiol. 51 (2010) 326–328.
[111] C. Senft, E. Hattingen, U. Pilatus, K. Franz, A. Schanzer, H. Lanfermann, V. Seifert, T. Gasser, Diagnostic value of proton Magnetic Resonance spectroscopy in the noninvasive grading of solid gliomas: comparison of maximum and mean choline values, Neurosurgery 65 (2009) 908–913.
[112] Q. Zeng, H. Liu, K. Zhang, C. Li, G. Zhou, Noninvasive evaluation of cerebral glioma grade by using multivoxel 3D proton MR spectroscopy, Magn. Reson. Imaging, 2010, doi:10.1016/j.mri.2010.07.017.
[113] H. Shimizu, T. Kumabe, T. Tominaga, T. Kayama, K. Hara, Y. Ono, K. Sato, N. Arai, S. Fujiwara, T. Yoshimoto, Noninvasive evaluation of malignancy of brain tumors with proton MR spectroscopy, AJNR Am. J. Neuroradiol. 17 (1996) 737–747.
[114] X. Li, Y. Lu, A. Pirzkall, T. McKnight, S.J. Nelson, Analysis of the spatial characteristics of metabolic abnormalities in newly diagnosed glioma patients, J. Magn. Reson. Imaging 16 (2002) 229–237.
[115] A. Panigrahy, M.D. Krieger, I. Gonzalez-Gomez, X. Liu, J.G. McComb, J.L. Finlay, M.D. Nelson Jr., F.H. Gilles, S. Blüml, Quantitative short echo time 1H-MR spectroscopy of untreated pediatric brain tumors: preoperative diagnosis and characterization, AJNR Am. J. Neuroradiol. 27 (2006) 560–572.
[116] E. Hattingen, P. Raab, K. Franz, H. Lanfermann, M. Setzer, R. Gerlach, F.E. Zanella, U. Pilatus, Prognostic value of choline and creatine in WHO grade II gliomas, Neuroradiology 50 (2008) 759–767.
[117] A. Stadlbauer, S. Gruber, C. Nimsky, R. Fahlbusch, T. Hammen, R. Buslei, B. Tomandl, E. Moser, O. Ganslandt, Preoperative grading of gliomas by using metabolite quantification with high-spatial-resolution proton MR spectroscopic imaging, Radiology 238 (2006) 958–969.
[118] A. Server, R. Josefsen, B. Kulle, J. Mæhlen, T. Schellhorn, Ø. Gadmar, T. Kumar, M. Haakonsen, C.W. Langberg, P.H. Nakstad, Proton magnetic resonance spectroscopy in the distinction of high-grade cerebral gliomas from single metastatic brain tumors, Acta Radiol. 51 (2010) 316–325.
[119] R. Hourani, L.J. Brant, T. Rizk, J.D. Weingart, P.B. Barker, A. Horska, Can proton MR spectroscopic and perfusion imaging differentiate between neoplastic and nonneoplastic brain lesions in adults? AJNR Am. J. Neuroradiol. 29 (2008) 366–372.
[120] M. Toyooka, H. Kimura, H. Uematsu, Y. Kawamura, H. Takeuchi, H. Itoh, Tissue characterization of glioma by proton magnetic resonance spectroscopy and perfusion-weighted magnetic resonance imaging: glioma grading and histological correlation, Clin. Imaging 32 (2008) 251–258.
[121] M.V. Spampinato, J.K. Smith, L. Kwock, M. Ewend, J.D. Grimme, D.L.A. Camacho, M. Castillo, Cerebral blood volume measurements and proton MR spectroscopy in grading of oligodendroglial tumors, AJR Am. J. Roentgenol. 188 (2007) 204–212.
[122] H. Yerli, A.M. Agildere, O. Ozen, E. Geyik, B. Atalay, A.H. Elhan, Evaluation of cerebral glioma grade by using normal side creatine as an internal reference in multi-voxel ^{1}H-MR spectroscopy, Diagn. Interv. Radiol. 13 (2007) 3–9.
[123] P. Zonari, P. Baraldi, G. Crisi, Multimodal MRI in the characterization of glial neoplasms: the combined role of single-voxel MR spectroscopy, diffusion imaging and echo-planar perfusion imaging, Neuroradiology 49 (2007) 795–803.
[124] J. Chen, S.-L. Huang, T. Li, X.-L. Chen, In vivo research in astrocytoma cell proliferation with ^{1}H-magnetic resonance spectroscopy: correlation with histopathology and immunohistochemistry, Neuroradiology 48 (2006) 312–318.
[125] J.-H. Kim, K.-H. Chang, D.G. Na, I.C. Song, B.J. Kwon, M.H. Han, K. Kim, 3T H-MR spectroscopy in grading of cerebral gliomas: comparison of short and intermediate echo time sequences, AJNR Am. J. Neuroradiol. 27 (2006) 1412–1418.
[126] P.C. Sundgren, MR spectroscopy in radiation injury, AJNR Am. J. Neuroradiol. 30 (2009) 1469–1476.
[127] A. Server, Response to a letter by Paul E. Sijens, Acta Radiol. 51 (2010) 329–333.
[128] T.R. McKnight, M.H. Von Dem Bussche, D.B. Vigneron, Y. Lu, M.S. Berger, M.W. McDermott, W.P. Dillon, E.E. Graves, A. Pirzkall, S.J. Nelson, Histopathological validation of a three-dimensional magnetic resonance spectroscopy index as a predictor of tumor presence, J. Neurosurg. 97 (2002) 794–802.
[129] T.R. McKnight, K.R. Lamborn, T.D. Love, M.S. Berger, S. Chang, W.P. Dillon, A. Bollen, S.J. Nelson, Correlation of magnetic resonance spectroscopic and growth characteristics within grades II and III gliomas, J. Neurosurg. 106 (2007) 660–666.
[130] J. Sabatier, V. Gilard, M. Malet-Martino, J.P. Ranjeva, C. Terral, S. Breil, M.B. Delisle, C. Manelfe, M. Tremoulet, I. Berry, Characterization of choline compounds with in vitro ^{1}H MRS for the discrimination of primary brain tumors, Invest. Radiol. 34 (1999) 230–235.
[131] V. Righi, O.C. Andronesi, D. Mintzopoulos, P.M. Black, A.A. Tzika, High-resolution magic angle spinning magnetic resonance spectroscopy detects glycine as a biomarker in brain tumors, Int. J. Oncol. 36 (2010) 301–306.
[132] G. Erb, K. Elbayed, M. Piotto, J. Raya, A. Neuville, M. Mohr, D. Maitrot, P. Kehrli, I.J. Namer, Toward improved grading of malignancy in oligodendrogliomas using metabolomics, Magn. Reson. Med. 59 (2008) 959–965.
[133] J. Sabatier, O. Robert, M.B. Delisle, M. Malet-Martino, Usefulness of in vitro ^{1}H magnetic resonance spectroscopy for the characterization of primary brain tumors: report of two cases, Stereot. Funct. Neurosurg. 83 (2005) 122–127.
[134] T. Beyer, B. Diehl, U. Holzgrabe, Quantitative NMR spectroscopy of biologically active substances and excipients, Bioanal. Rev. 2 (2010) 1–22.
[135] I. Wawer, Solid-State measurements of drugs and drug formulations, in: U. Holzgrabe, I. Wawer, B. Diehl (Eds.), NMR Spectroscopy in Pharmaceutical Analysis, Elsevier, Amsterdam, 2008, pp. 201–232.
[136] B.W.K. Diehl, ^{31}P-NMR in phospholipid analysis, Lipid Technol. 14 (2002) 62–65.
[137] Chap. 2.2.56, European Pharmacopoeia, 7th edition, Council of Europe, Strasbourg, 2010.
[138] U. Holzgrabe, C.-J. Nap, T. Beyer, S. Almeling, Alternatives to amino-acid-analysis for the purity control of pharmaceutical grade L-alanine, J. Sep. Sci. 33 (2010) 2402–2410.
[139] E. Kellenbach, K. Sanders, G. Zomer, P.L.A. Overbeeke, The use of proton NMR as an alternative for the amino acid analysis as identity test for peptides, Pharm. Sci. Notes 1 (2008) 1–7.
[140] C.W. Funke, J.R. Mellema, P. Saleminik, G.N. Wagenaars, The discrimination between human, porcine and bovine insulin with ^{1}H NMR spectroscopy, J. Pharm. Pharmacol. 40 (1988) 78–79.
[141] J.A. Goncalves, S. Ahuja, S. Erfani, M. Eilers, S.O. Smith, Structure and function of G protein-coupled receptors using NMR spectroscopy, Progr. NMR Spectrosc. 57 (2010) 159–180.

[142] M. Guerrini, D. Beccati, Z. Shriver, A. Naggi, K. Viswanathan, A. Bisio, I. Capila, J.C. Lansing, S. Guglieri, B. Fraser, A. Al-Hakim, N. Sibel Gunay, Z. Zhang, L. Robinson, L. Buhse, M. Nasr, J. Woodcock, R. Langer, G. Venkataraman, R.J. Linhardt, B. Casu, G. Torri, R. Sasikheran, Oversulfated chondroitin sulfate is a contaminant in heparin associated with adverse clinical events, Nat. Biotechnol. 26 (2008) 669–675.
[143] T. Beyer, B. Diehl, G. Randel, E. Humpfer, H. Schäfer, M. Spraul, C. Schollmayer, U. Holzgrabe, Quality assessment of unfractionated heparin using ^{1}H nuclear magnetic resonance spectroscopy, J. Pharm. Biomed. Anal. 48 (2008) 13–19.
[144] I. McEwen, A. Amini, I.M. Olofsson, Identification and purity test of heparin by NMR – a summary of two years' experience at the Medical Products Agency, Pharm. Bio. Sci. Notes 1 (2010) 65–72.
[145] S.E. Lee, E.K. Chess, B. Rabinow, G.J. Ray, C.M. Szabo, B. Melnick, R.L. Miller, L.M. Nair, E.G. Moore, NMR of heparin API: investigation of unidentified signals in the USP-specified range of 2.12–3.00 ppm, Anal. Bioanal. Chem. 399 (2011) 651–662.
[146] P.A.J. Mourier, O.Y. Guichard, F. Herman, C. Viskov, Heparin sodium compliance to the new proposed USP monograph: elucidation of a minor structural modification responsible for a process dependent 2.10 ppm NMR signal, J. Pharm. Biomed. Anal. 54 (2011) 337–344.
[147] Q. Zang, D.A. Keire, R.D. Wood, L.F. Buhse, C.M.V. Moore, M. Nasr, A. Al-Hakim, M.L. Trehy, W.J. Welsh, Determination of galactosamine impurities in heparin samples by multivariate regression analysis of their ^{1}H NMR spectra, Anal. Bioanal. Chem. 399 (2011) 635–649.
[148] B. Üstün, K.B. Sanders, P. Dani, E. Kellenbach, Quantification of chondroitin sulfate and dermatan sulfate in danaparoid sodium by ^{1}H NMR spectroscopy and PLS regression, Anal. Bioanal. Chem. 399 (2011) 629–634.
[149] T.K.N. Nguyen, Y.M. Tran, X.V. Victor, J.J. Skalicky, B. Kuberan, Characterization of uniformly and atom-specifically ^{13}C-labeled heparin and heparin sulfate polysaccharide precursor using ^{13}C NMR spectroscopy and ESI mass spectrometry, Carbohydr. Res. 345 (2010) 2228–2232.
[150] J.F.K. Limtiaco, S. Beni, C.J. Jones, D.J. Langeslay, C.K. Larive, NMR methods to monitor the enzymatic depolymerization of heparin, Anal. Bional. Chem. 399 (2011) 593–603.